CPT: Pharmacometrics & Systems Pharmacology

Supplementary Material: A Physiologically-Based Pharmacokinetic Precision Dosing Approach to Manage Dasatinib Drug–Drug Interactions

Christina Kovar[1,2], Helena Leonie Hanae Loer[1], Simeon Rüdesheim[1,2], Laura Maria Fuhr[1], Fatima Zahra Marok[1], Dominik Selzer[1], Matthias Schwab[2,3,4] and Thorsten Lehr[1]

[1]Clinical Pharmacy, Saarland University, Saarbrücken, Germany
[2]Dr. Margarete Fischer-Bosch Institute of Clinical Pharmacology, Stuttgart, Germany
[3]Departments of Clinical Pharmacology, and Pharmacy and Biochemistry, University of Tübingen, Tübingen, Germany
[4]Cluster of Excellence iFIT (EXC2180), Image-Guided and Functionally Instructed Tumor Therapies, University of Tübingen, Tübingen, Germany

Funding
Matthias Schwab was supported by the Robert Bosch Stiftung (Stuttgart, Germany), a grant from the German Federal Ministry of Education and Research (BMBF, 031L0188D, "GUIDE-IBD") and the DFG im Rahmen der Exzellenzstrategie des Bundes und der Länder-EXC 2180-390900677. Thorsten Lehr was supported by the German Federal Ministry of Education and Research (BMBF, Horizon 2020 INSPIRATION grant 643271), under the frame of ERACoSysMed and the European Union Horizon 2021 SafePolyMed (grant 101057639).

Conflict of Interest
The authors declared no competing interests for this work.

Corresponding Author
Prof. Dr. Thorsten Lehr
Clinical Pharmacy, Saarland University
Campus C5 3, 66123 Saarbrücken, Germany
ORCID: 0000-0002-8372-1465
Phone: +49 681 302 70255
Email: thorsten.lehr@mx.uni-saarland.de

Contents

S1 PBPK Model Building

S1.1 Assignment to Training and Test Dataset

Plasma profiles from the literature were divided into a training and a test dataset for model building (5 profiles) and evaluation (58 profiles), respectively. The plasma profiles were allocated to the training and test datasets using a non-randomized strategy to ensure comprehensive and varied data for model building. This data assortment encapsulated a wide spectrum of dosing ranges and an array of dosing regimens. In the process, we strived to maximize the number of plasma profiles for model evaluation. We specifically selected datasets with dense sampling intervals spanning a prolonged investigation period for the training dataset. An overview of all clinical studies is presented in Table S1, Table S7 and Table S9.

S1.2 Virtual Individuals

Virtual "mean individuals" were created for each study based on mean or mode of age, sex, body weight, height, body mass index and ethnicity from the corresponding study reports. If demographic information was not provided for a study, either a 30-year-old white American male with a body weight of 80 kg and height of 1.78 m for healthy volunteers or a 64-year-old white American male with body weight of 82 kg and height of 1.75 m for cancer patients were used according to the third National Health and Nutrition Examination Survey (NHANES) database [1].
For each compartment expressing cytochrome P450 3A4 (CYP3A4), we applied uniform parameter values for the Michaelis-Menten kinetics—specifically, the Michaelis constant (K_m) and the catalytic constant (k_{cat})—to model CYP3A4-mediated metabolism. In general, enzyme and transporter expressions in different tissues were implemented according to the PK-Sim® expression database.
As CML is more prevalent in men, with an average diagnosis age of 64 years, a virtual 64-year-old European male individual was used for the dosing simulations [2]. Default values for body weight (64 kg) and height (1.70 m) were derived from the International Commission on Radiological Protection (ICRP) database [3].

S1.3 Virtual Populations

Virtual populations of 100 individuals were generated based on the respective study population demographics. Depending on the ethnicity and demographic characteristics, virtual individuals were varied by the implemented algorithm in PK-Sim® within the limits of the NHANES database for white Americans, the ICRP database for Europeans and the integrated database for Japanese population [4]. The corresponding algorithms for the generation of virtual populations have been reported by Willmann and coworkers [5].
For the studies CA180016 [6] and CA180032 [6] as well as the studies by Christopher et al. 2008 (a) [7], Vaidhyanathan et al. 2019 [8] and Vargas et al. 2016 [9] an age range of 20 to 50 years for healthy volunteers was assumed, while for the studies CA180005 and CA180009 as well as the studies by Christopher et al. 2008 (b) [7] and Luo et al. 2008 [10] an age range of 20 to 80 years for cancer patients was used since information about the study populations were not available. System-dependent parameters including reference concentrations and enzyme expression variabilities are listed in Table S2.

S1.4 Clinical Studies

Table S1: Overview of clinical study data from the literature used for model development.

Clinical study	Dose [mg]	Route	N	Females [%]	Age [years]	Weight [kg]	BMI [kg/m²]	Gastric pH	Fasted/ Fed	Health Status	Dataset
Bioequivalence study [13]	140	po, tab, sd	122	-	- (18–48)	-	24.1 (-)[a]	2.0[b]	fasted	healthy	training
Christopher 2008 (a) [7]	100	po, sol, sd	8	0	-	-	-	2.0[b]	-[c]	healthy	test
Furlong 2012 [14]	100	po, tab, sd	20	-	-	-	-	2.0[b]	fasted	healthy	training
Study CA180016 [6]	100	po, tab, sd	18	-	-	-	-	2.0[b]	-[c]	healthy	test
Vaidhyanathan 2018 (a) [8]	70	po, tab, sd	64	-	-	-	-	2.0[b]	fasted	healthy	training
Vaidhyanathan 2018 (b) [8]	100	po, PFOS, sd	-	-	-	-	-	2.0[b]	fasted	healthy	test
Vaidhyanathan 2018 (c) [8]	100	po, dispersed tab, sd	-	-	-	-	-	2.0[b]	fasted	healthy	test
Vaidhyanathan 2018 (d) [8]	100	po, tab, sd	-	-	-	-	-	2.0[b]	fasted	healthy	test
Vargas 2016 [9]	100	po, tab, sd	-	-	28 (-)[a]	65 (-)[a]	22.7 (-)[a]	2.0[b]	fasted	healthy	test
Araujo 2012 [15]	100	po, tab, qd, md	46	0	65 (48–83)[d,e]	-	-	2.0[b]	-[c]	cancer	test
Christopher 2008 (b) [7]	180	po, tab, sd	3	-	-	-	-	2.0[b]	-[c]	cancer	test
Demetri 2009 (a) [16]	35	po, tab, bid, md (B5D)	4	39.4[g]	56 (32–81)[d,g]	-	-	2.0[b]	fasted	cancer	test
Demetri 2009 (b) [16]	50	po, tab, bid, md (B5D)	3	39.4[g]	56 (32–81)[d,g]	-	-	2.0[b]	fasted	cancer	test
Demetri 2009 (c) [16]	70	po, tab, bid, md (B5D)	4	39.4[g]	56 (32–81)[d,g]	-	-	2.0[b]	fasted	cancer	test
Demetri 2009 (d) [16]	70	po, tab, bid, md (B7D)	3	47.1[g]	59 (31–82)[d,g,e]	-	-	2.0[b]	fasted	cancer	test
Demetri 2009 (e) [16]	90	po, tab, bid, md (B5D)	5	39.4[g]	56 (32–81)[d,g]	-	-	2.0[b]	fasted	cancer	test
Demetri 2009 (f) [16]	90	po, tab, bid, md (B7D)	5	47.1[g]	59 (31–82)[d,g,e]	-	-	2.0[b]	fasted	cancer	test
Demetri 2009 (g) [16]	100	po, tab, bid, md (B7D)	7	47.1[g]	59 (31–82)[d,g,e]	-	-	2.0[b]	fasted	cancer	test
Demetri 2009 (h) [16]	120	po, tab, bid, md (B5D)	7	39.4[g]	56 (32–81)[d,g]	-	-	2.0[b]	fasted	cancer	test
Demetri 2009 (i) [16]	120	po, tab, bid, md (B7D)	1	47.1[g]	59 (31–82)[d,g,e]	-	-	2.0[b]	fasted	cancer	test
Demetri 2009 (j) [16]	160	po, tab, bid, md (B5D)	1	39.4[g]	56 (32–81)[d,g]	-	-	2.0[b]	fasted	cancer	test
Luo 2008 [10]	90	po, tab, bid, md	-	-	-	-	-	2.0[b]	-[c]	cancer	test
Study CA180002 (a) [6]	15	po, tab, qd, md (Q5D)	3	-	56 (15–79)[d,f]	-	-	2.0[b]	fasted	cancer	test
Study CA180002 (b) [6]	25	po, tab, bid, md (B5D)	3	-	56 (15–79)[d,f]	-	-	2.0[b]	fasted	cancer	test
Study CA180002 (c) [6]	30	po, tab, qd, md (Q5D)	3	-	56 (15–79)[d,f]	-	-	2.0[b]	fasted	cancer	test
Study CA180002 (d) [6]	35	po, tab, bid, md (B5D)	8	-	56 (15–79)[d,f]	-	-	2.0[b]	fasted	cancer	test
Study CA180002 (e) [6]	50	po, tab, bid, md (B5D)	3–5	-	56 (15–79)[d,f]	-	-	2.0[b]	fasted	cancer	test
Study CA180002 (f) [6]	50	po, tab, bid, md (B7D)	6–8	-	56 (15–79)[d,f]	-	-	2.0[b]	fasted	cancer	test
Study CA180002 (g) [6]	50	po, tab, qd, md (Q5D)	3	-	56 (15–79)[d,f]	-	-	2.0[b]	fasted	cancer	test

-: unknown, **B5D**: five consecutive days bid dosing followed by two nontreatment days, **B7D**: continuous bid dosing, **bid**: twice a day, **BMI**: body mass index, **md**: multiple dose, **N**: number of participants, **PFOS**: powder for oral suspension, **po**: peroral, **Q5D**: five consecutive days once daily dosing followed by two nontreatment days, **qd**: once a day, **sd**: single dose, **sol**: solution, **tab**: tablet

[a] Mean (range)
[b] Default value in PK-Sim® for fasted state [11]
[c] A light-fat breakfast or fasted state was assumed
[d] Median (range)
[e] Maximum age of the NHANES database is 81 years [1]
[f] Values refer to the whole study population
[g] Values refer to the whole study population (stratified by regimen)
[h] Assumed (based on the reported age range of 12–17 [12])

Table S1: Overview of clinical study data from the literature used for model development *(continued)*.

Clinical study	Dose [mg]	Route	N	Females [%]	Age [years]	Weight [kg]	BMI [kg/m²]	Gastric pH	Fasted/ Fed	Health Status	Dataset
Study CA180002 (h) [6]	70	po, tab, bid, md (B5D)	6–9	-	56 (15–79)[d,f]	-	-	2.0[b]	fasted	cancer	test
Study CA180002 (i) [6]	70	po, tab, bid, md (B7D)	11–14	-	56 (15–79)[d,f]	-	-	2.0[b]	fasted	cancer	test
Study CA180002 (j) [6]	75	po, tab, qd, md (Q5D)	3	-	56 (15–79)[d,f]	-	-	2.0[b]	fasted	cancer	test
Study CA180002 (k) [6]	90	po, tab, bid, md (B7D)	11	-	56 (15–79)[d,f]	-	-	2.0[b]	fasted	cancer	test
Study CA180002 (l) [6]	105	po, tab, qd, md (Q5D)	3	-	56 (15–79)[d,f]	-	-	2.0[b]	fasted	cancer	test
Study CA180002 (m) [6]	120	po, tab, bid, md (B7D)	7	-	56 (15–79)[d,f]	-	-	2.0[b]	fasted	cancer	test
Study CA180002 (n) [6]	140	po, tab, qd, md (Q5D)	3	-	56 (15–79)[d,f]	-	-	2.0[b]	fasted	cancer	test
Study CA180002 (o) [6]	180	po, tab, qd, md (Q5D)	3	-	56 (15–79)[d,f]	-	-	2.0[b]	fasted	cancer	test
Study CA180005 (a) [6]	70	po, tab, bid, md (B5D)	-	-	-	-	-	2.0[b]	-[c]	cancer	test
Study CA180005 (b) [6]	70	po, tab, bid, md (B7D)	-	-	-	-	-	2.0[b]	-[c]	cancer	test
Takahashi 2011 (a) [17]	100	po, tab, qd, md	9	77.8	58 (33–65)[d]	-	-	2.0[b]	fed[c]	cancer	test
Takahashi 2011 (b) [17]	150	po, tab, qd, md	3	33.3	55 (39–63)[d]	-	-	2.0[b]	fed[c]	cancer	test
Takahashi 2011 (c) [17]	200	po, tab, qd, md	4	75.0	47.5 (33–53)[d]	-	-	2.0[b]	fed[c]	cancer	test
Zwaan 2013 (a) [12]	100	po, tab, qd, sd	9	-	15[h] (12–17)	-	-	2.0[b]	-[c]	cancer	test
Zwaan 2013 (b) [12]	140	po, tab, qd, sd	8	-	15[h] (12–17)	-	-	2.0[b]	-[c]	cancer	test
Zwaan 2013 (c) [12]	170	po, tab, qd, sd	9	-	15[h] (12–17)	-	-	2.0[b]	-[c]	cancer	test
Zwaan 2013 (d) [12]	200	po, tab, qd, sd	2	-	15[h] (12–17)	-	-	2.0[b]	-[c]	cancer	test

-: unknown, **B5D**: five consecutive days bid dosing followed by two nontreatment days, **B7D**: continuous bid dosing, **bid**: twice a day, **BMI**: body mass index, **md**: multiple dose, **N**: number of participants, **PFOS**: powder for oral suspension, **po**: peroral, **Q5D**: five consecutive days once daily dosing followed by two nontreatment days, **qd**: once a day, **sd**: single dose, **sol**: solution, **tab**: tablet

[a] Mean (range)
[b] Default value in PK-Sim® for fasted state [11]
[c] A light-fat breakfast or fasted state was assumed
[d] Median (range)
[e] Maximum age of the NHANES database is 81 years [1]
[f] Values refer to the whole study population
[g] Values refer to the whole study population (stratified by regimen)
[h] Assumed (based on the reported age range of 12–17 [12])

S1.5 System-dependent Parameters

Table S2: System-dependent parameters and expression of relevant enzymes, transporters and processes.

Enzyme/Transporter/ Processes	Mean ref. conc. [µmol/L][a]	GeoSD of the ref. conc.[b]	Relative expression in different organs[c]	Half-life liver [hours]	Half-life intestine [hours]
AADAC	1.00[d] [18]	1.40[e]	RT-PCR [26]	36	23
CYP1A2	1.80 [27]	1.63 (liver) [28]	RT-PCR [29]	39	23
CYP2A6	2.72 [27]	1.40[e]	RT-PCR [29]	26	23
CYP2B6	1.56 [27]	1.40[e]	RT-PCR [29]	32	23
CYP2C19	0.76 [27]	1.79 (liver) [28]	RT-PCR [29]	26	23
CYP2C8	2.56 [27]	2.05 (liver) [28]	RT-PCR [29]	23	23
CYP2D6	0.40 [27]	2.49 [28]	RT-PCR [29]	51	23
CYP3A4	4.32 [27]	1.18/1.46 (liver/duodenum) [28]	RT-PCR [29]	36 [30]	23 [31]
CYP3A5	0.04 [18]	1.40[e]	RT-PCR [29]	36	23
EPHX1	1.00[d] [18]	1.40[e]	RT-PCR [26]	36	23
FMO3	1.00[d]	1.00 [18]	RT-PCR [26]	-	23
PON3	1.00[d]	1.40[e]	Array [29]	36	23
UGT1A1	1.00[d]	1.40[e]	RT-PCR [26]	36	23
UGT1A3	1.00[d]	1.40[e]	RT-PCR [26]	36	23
UGT1A4	2.32[f]	1.07[28]	RT-PCR [26]	36	23
UGT2B7[g]	2.78[f] [32]	1.60 (liver) [28]	EST [33]	36	23
Unspecific liver lactonization	1.00[d]	1.40[e]	Liver only	36	23
Unspecific plasma hydrolysis	1.00[d]	1.40[e]	Plasma only	36	23
BCRP	1.00[d]	1.35 [34]	RT-PCR[h] [35]	36	23
MRP2	1.00[d]	1.49 [36]	Array [37]	36	23
OATP1B1	0.07[i,j] [23]	1.54 [23]	RT-PCR [35]	36	-
OATP1B3	1.00[d] [18]	1.54 [23]	Array [37]	36	23
P-gp	1.41[optimized]	1.60 [23]	RT-PCR[k] [35]	36	23
Unspecific liver influx	1.00[d]	1.40[e]	Liver only	36	23
Unspecific hepatic clearance	-	-			
Chemical hydrolysis	1.00	-	Ubiquitous	36	23

AADAC: arylacetamide deacetylase, **BCRP**: breast cancer resistance protein, **CYP**: cytochrome P450, **EST**: espressed sequence tag, **EPHX1**: epoxide hydroxylase 1, **FMO**: flavin-containing monooxygenase, **GeoSD**: geometric standard deviation, **MRP2**: multidrug resistance-associated protein 2, **OATP**: organic anion transporting polypeptide, **P-gp**: P-glycoprotein, **PON3**: paraoxonase 3, **ref. conc.**: reference concentration, **RT-PCR**: reverse transcription polymerase chain reaction, **UGT**: UDP-glucuronosyltransferase

[a] μmol protein/L in the tissue of highest expression
[b] Geometric standard deviation of the reference concentration
[c] In the different organs (PK-Sim® expression database profile)
[d] If no information was available, the mean ref. conc. was set to 1.0 μmol/L and the catalytic rate constant (k_{cat}) was optimized according to [18]
[e] If no information was available a moderate variability of 35% CV was assumed (= 1.40 GSD)
[f] Calculated from protein per mg microsomal protein × 40.0 mg microsomal protein per g liver [19]
[g] UGT2B7 enzyme for metabolism of fluconazole and simvastatin was implemented according to the respective publication [20, 21]
[h] With relative expression in blood cells set to 0.3046 [22]
[i] Calculated from transporter per mg membrane protein × 37.0 mg membrane protein per g liver [23]
[j] Differences in the implementation of the OATP1B1 ref. conc. in the rifampicin [24], simvastatin [21] and erythromycin [25] PBPK model were compensated by using the concentration of 0.07 μmol/L [23] and optimizing the k_{cat}
[k] With relative expression in intestinal mucosa increased by factor 3.57 [24]

Table S3: Relative enzymes and transporters expression in organs and tissues implemented in the dasatinib PBPK model [%]

	CYP2C8	**CYP3A4**	**OATP1B1**	**OATP1B3**
Data source	RT-PCR [29]	RT-PCR [29]	RT-PCR [35]	Array [37]
Blood cells	0	0	0	0
Plasma	0	0	-	-
Bone	0	0	0	3
Brain	0	0	0	3
Fat	0	0	0	0
Gonads	1	0	1	4
Heart	0	0	0	6
Kidney	0	1	0	2
Liver periportal	100	100	100	100
Liver pericentral	100	100	100	100
Lung	0	0	0	2
Muscle	0	0	0	2
Pancreas	0	0	0	1
Skin	0	0	0	1
Spleen	0	0	0	1
Duodenum mucosa	0	7	0	2
Upper jejunum mucosa	0	7	0	2
Lower jejunum mucosa	0	7	0	2
Upper ileum mucosa	0	7	0	2
Lower ileum mucosa	0	7	0	2
Cecum mucosa	0	0	0	0
Colon ascendens mucosa	0	0	0	1
Colon transversum mucosa	0	0	0	1
Colon descendens mucosa	0	0	0	1
Colon sigmoid mucosa	0	0	0	1
Rectum mucosa	0	0	0	0
Stomach non-mucosal tissue	0	0	0	1
Small intestine non-mucosal tissue	0	7	0	2
Large intestine non-mucosal tissue	0	0	0	1
Stomach lumen	0	0	-	-
Duodenum lumen	0	0	-	-
Upper jejunum lumen	0	0	-	-
Lower jejunum lumen	0	0	-	-
Upper ileum lumen	0	0	-	-
Lower ileum lumen	0	0	-	-
Cecum lumen	0	0	-	-
Colon ascendens lumen	0	0	-	-
Colon transversum lumen	0	0	-	-
Colon descendens lumen	0	0	-	-
Colon sigmoid lumen	0	0	-	-
Rectum lumen	0	0	-	-

Array: microarray expression profile, **CYP**: cytochrome P450, **OATP**: organic anion transporting polypeptide

S1.6 Drug-dependent Parameter Table

Table S4: Drug-dependent parameters for dasatinib.

Parameter	Value [95% CI]	Unit	Source	Literature	Reference	Description
MW	488.01	g/mol	Literature	488.01	[39]	Molecular weight
pK_a (base)	3.10, 6.80	-	Literature	3.10, 6.80	[40]	Acid dissociation constant
pK_a (acid)	10.80	-	Literature	10.80	[40]	Acid dissociation constant
Solubility (pH 4.0)	0.04	mg/ml	Literature	0.04	[41]	Solubility
logP	3.59 [3.47, 3.71]	-	Optimized	2.71–4.01	[39, 40]	Lipophilicity
f_u	4.00	%	Literature	4.00	[42]	Fraction unbound
CYP3A4 K_m → M20[a]	6.00	µmol/l	Literature	6.00	[43]	Michaelis-Menten constant
CYP3A4 k_{cat} → M20[a]	58.38 [46.19, 70.57]	1/min	Optimized	-	-	Catalytic rate constant
CYP3A4 K_I	9.00	µmol/l	Literature	9.00	[44]	Inhibition Constant
CYP3A4 k_{inact}	0.02	1/min	Literature	0.02	[44]	Maximum rate of inactivation
CYP2C8 K_i	3.60	µmol/l	Literature	3.60	[44]	Dissociation Constant
OATP1B1 K_i	2.33	µmol/l	Literature	2.33	[45]	Dissociation Constant
OATP1B3 K_i	2.75	µmol/l	Literature	2.75	[45]	Dissociation Constant
Unspecific hepatic clearance	5.62 [3.17, 8.07]	1/min	Optimized	-	-	Elimination from plasma (first-order process in the liver)
GET (fasted)	15.00	min	Literature	15.00	[46]	Gastric emptying time
GET (fed)	103.44	min	Optimized	45–120	[47]	Gastric emptying time
GET (with Rabeprazole)	60.13	min	Optimized	-	-	Gastric emptying time
GET (with Maalox®)	31.27	min	Optimized	-	-	Gastric emptying time
GFR fraction	1.00	-	Assumed	-	-	Fraction of filtered drug in the urine
EHC continuous fraction	1.00	-	Assumed	-	-	Fraction of bile continually released
Partition coefficients	Diverse[b]	-	Calculated	Schmitt	[48]	Cell to plasma partition coefficients
Cellular permeability	Diverse[b]	cm/min	Calculated	PK-Sim Standard	[46]	Permeability into the cellular space
Intestinal permeability	$1.22 \cdot 10^{-6}$ [$6.42 \cdot 10^{-7}$, $1.80 \cdot 10^{-6}$]	cm/s	Optimized	-	-	Transcellular intestinal permeability
Density	1.41	g/cm^3	Literature	1.41	[49]	Density
Aqueous diffusion coefficient	$2.67 \cdot 10^{-4}$	cm^2/min	Calculated	$2.67 \cdot 10^{-4}$	-	Aqueous diffusion coefficient
Particle dissolution radius (Bin1)	11.46	µm	Calculated	11.46[c]	[8]	Mean Particle Radius
Particle dissolution radius (Bin2)	38.07	µm	Calculated	38.07[c]	[8]	Mean Particle Radius
Particle dissolution radius (Bin3)	67.86	µm	Calculated	67.86[c]	[8]	Mean Particle Radius

CI: confidence interval, **CYP**: cytochrome P450, **EHC**: enterohepatic circulation, **GFR**: glomerular filtration rate, **OATP**: organic anion transporting polypeptide

[a] Metabolite was not included in the PBPK model
[b] Values differ across the organs
[c] Calculated according to [38]

S2 PBPK Model Evaluation

S2.1 Healthy Volunteers

S2.1.1 Plasma Profiles (Linear Scale)

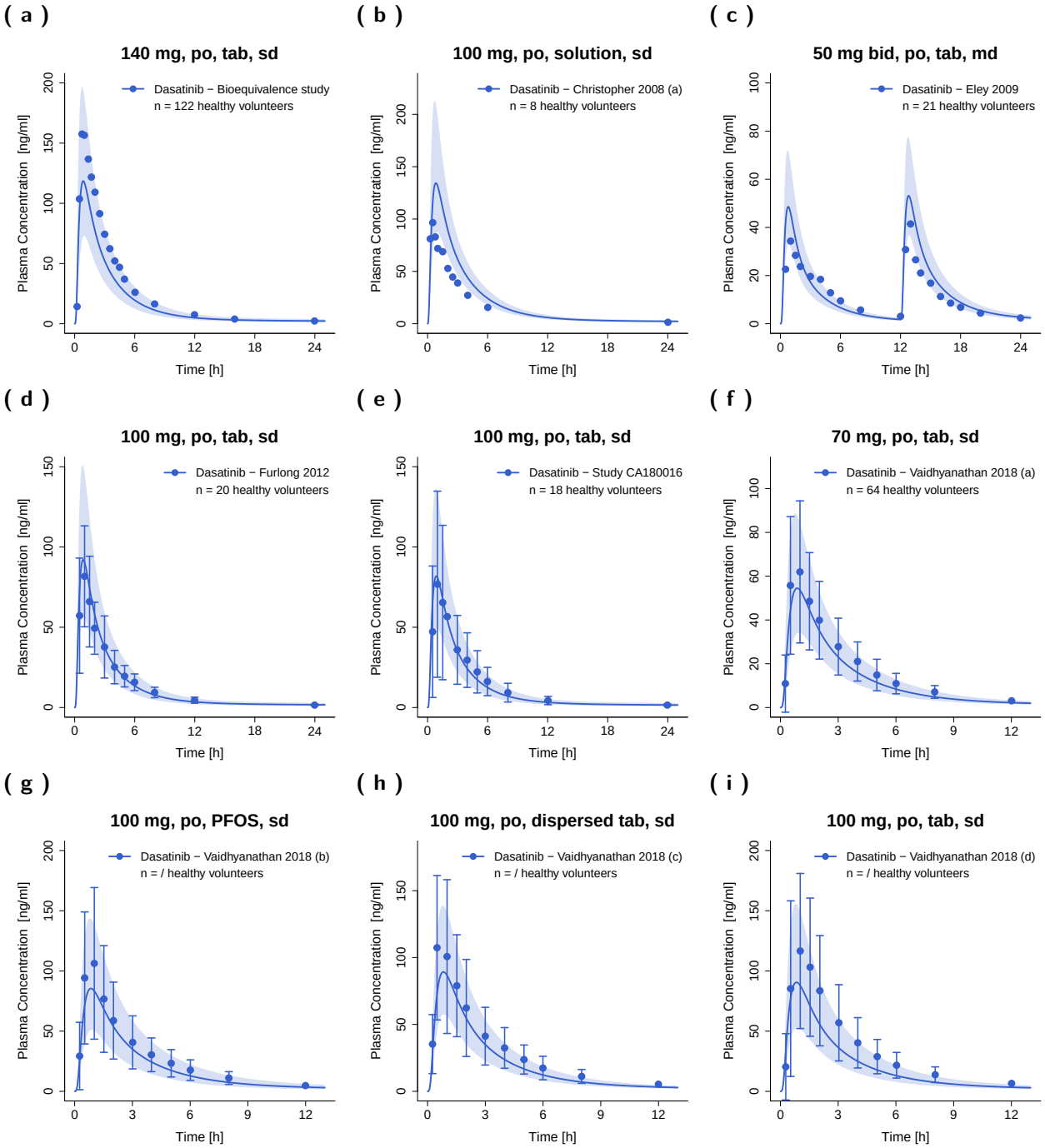

Figure S1: Predicted and observed dasatinib plasma concentration–time profiles in healthy volunteers on a linear scale. Solid lines show predicted geometric mean concentration–time profiles with ribbons illustrating the corresponding geometric standard deviation of the population simulations (n=100). Points demonstrate the mean observed data with the corresponding standard deviation of dasatinib (if depicted in the respective publication). /: no information available, **bid**: twice a day, **md**: multiple dose, **n**: number of participants, **PFOS**: powder for oral suspension, **po**: peroral, **qd**: once a day, **sd**: single dose, **tab**: tablet.

(j)

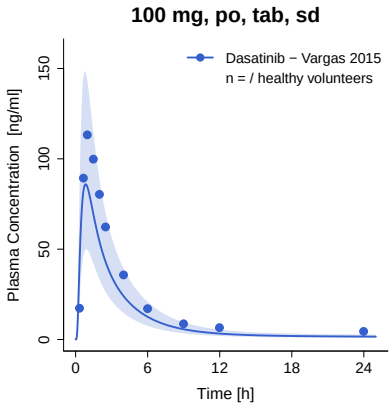

Figure S1: (*continued*) **Predicted and observed dasatinib plasma concentration–time profiles in healthy volunteers on a linear scale.** Solid lines show predicted geometric mean concentration–time profiles with ribbons illustrating the corresponding geometric standard deviation of the population simulations (n=100). Points demonstrate the mean observed data with the corresponding standard deviation of dasatinib (if depicted in the respective publication). /: no information available, **bid**: twice a day, **md**: multiple dose, **n**: number of participants, **PFOS**: powder for oral suspension, **po**: peroral, **qd**: once a day, **sd**: single dose, **tab**: tablet.

S2.1.2 Plasma Profiles (Semilogarithmic Scale)

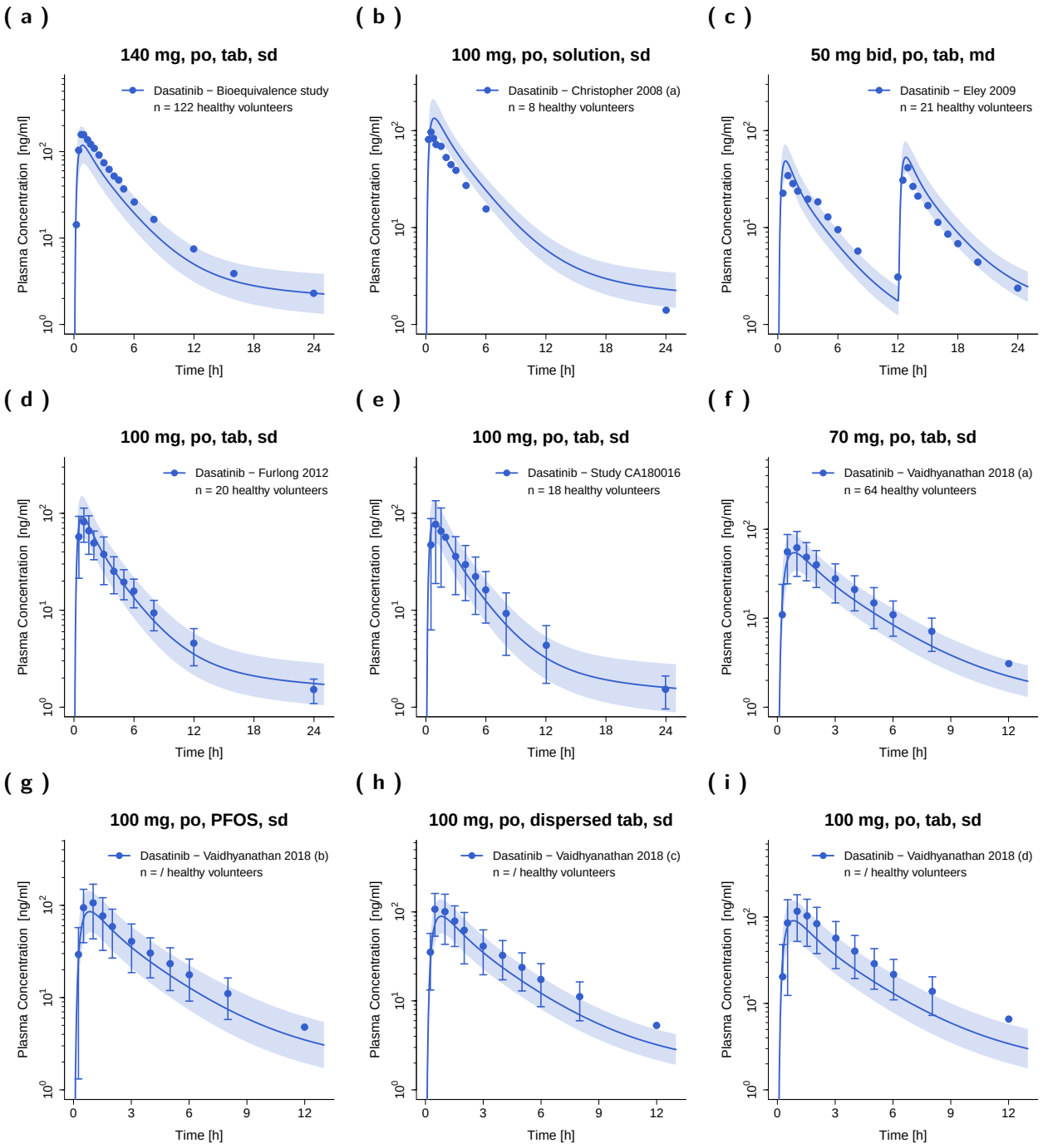

Figure S2: Predicted and observed dasatinib plasma concentration–time profiles in healthy volunteers on a semilogarithmic scale. Solid lines show predicted geometric mean concentration–time profiles with ribbons illustrating the corresponding geometric standard deviation of the population simulations (n=100). Points demonstrate the mean observed data with the corresponding standard deviation of dasatinib (if depicted in the respective publication). /: no information available, **bid**: twice a day, **md**: multiple dose, **n**: number of participants, **PFOS**: powder for oral suspension, **po**: peroral, **qd**: once a day, **sd**: single dose, **tab**: tablet.

(j)

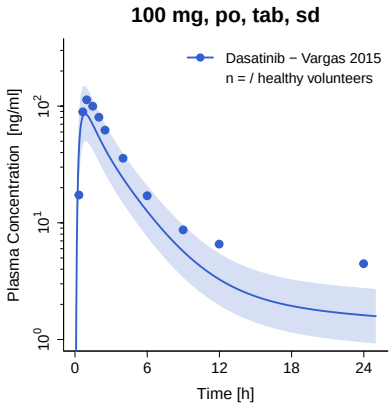

Figure S2: (*continued*) **Predicted and observed dasatinib plasma concentration–time profiles in healthy volunteers on a semilogarithmic scale.** Solid lines show predicted geometric mean concentration–time profiles with ribbons illustrating the corresponding geometric standard deviation of the population simulations (n=100). Points demonstrate the mean observed data with the corresponding standard deviation of dasatinib (if depicted in the respective publication). /: no information available, **bid**: twice a day, **md**: multiple dose, **n**: number of participants, **PFOS**: powder for oral suspension, **po**: peroral, **qd**: once a day, **sd**: single dose, **tab**: tablet.

S2.2 Cancer Patients

S2.2.1 Plasma Profiles (Linear Scale)

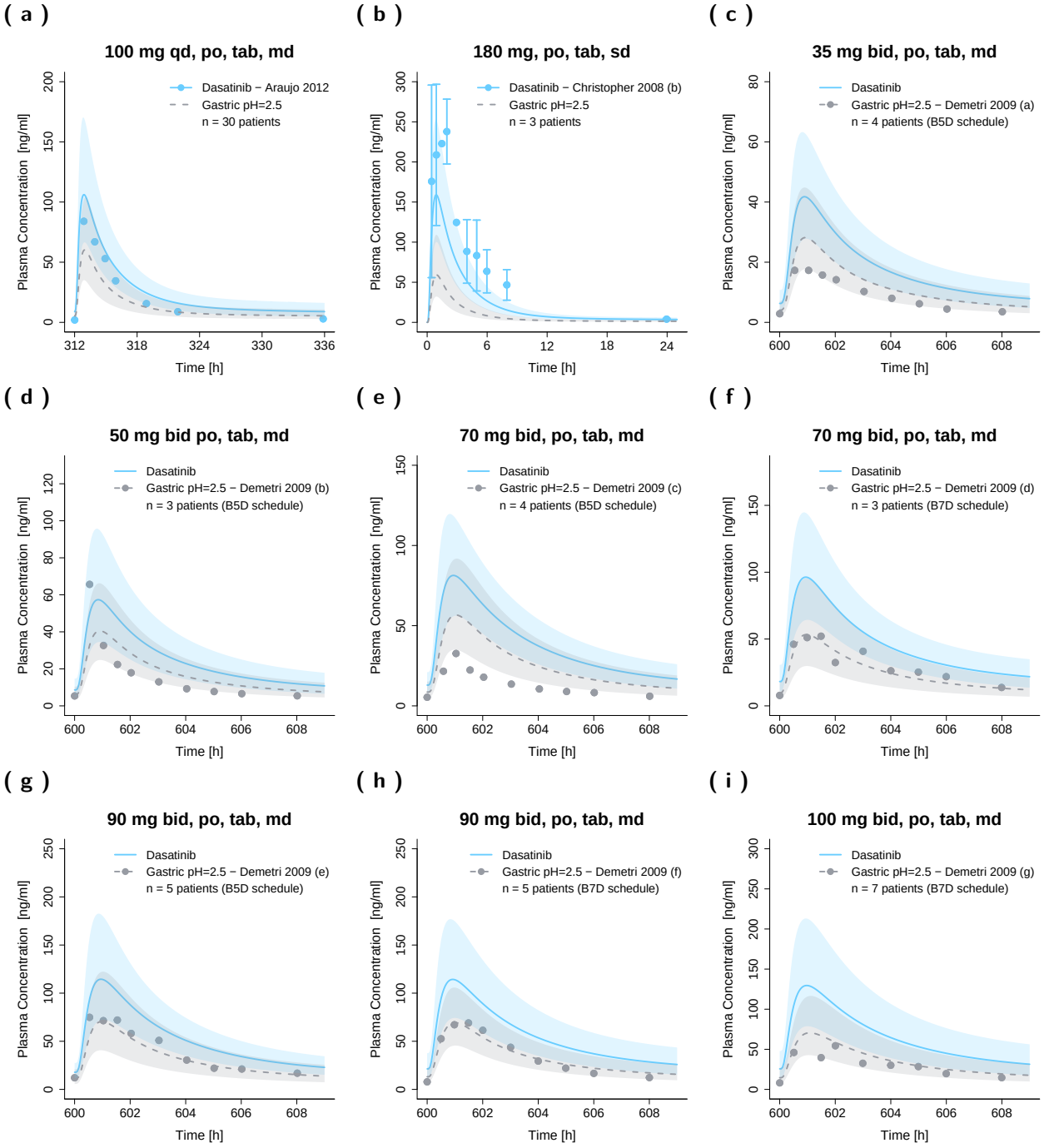

Figure S3: Predicted and observed dasatinib plasma concentration–time profiles in cancer patients on a linear scale. Solid and dashed lines show predicted geometric mean concentration–time profiles with gastric pH of 2.0 and 2.5, respectively, with ribbons illustrating the corresponding geometric standard deviation of the population simulations (n=100). Points demonstrate the mean observed data with the corresponding standard deviation of dasatinib (if depicted in the respective publication). /: no information available, **B5D**: five consecutive days bid dosing followed by two nontreatment days, **B7D**: seven consecutive days bid dosing, **bid**: twice a day, **md**: multiple dose, **n**: number of participants, **po**: peroral, **Q5D**: five consecutive days once daily dosing followed by two nontreatment days, **qd**: once a day, **sd**: single dose, **tab**: tablet.

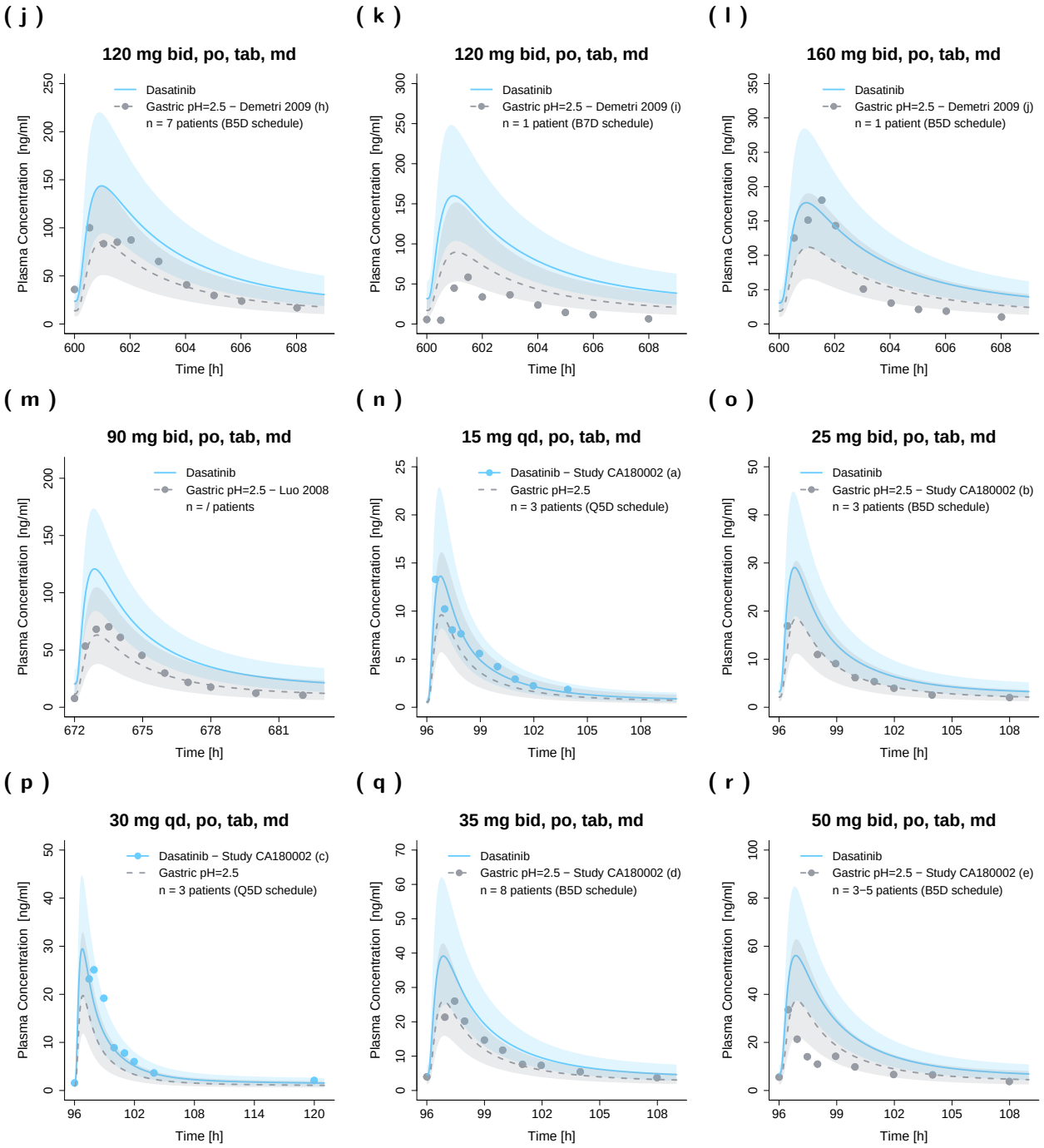

Figure S3: (*continued*) **Predicted and observed dasatinib plasma concentration–time profiles in cancer patients on a linear scale.** Solid and dashed lines show predicted geometric mean concentration–time profiles with gastric pH of 2.0 and 2.5, respectively, with ribbons illustrating the corresponding geometric standard deviation of the population simulations (n=100). Points demonstrate the mean observed data with the corresponding standard deviation of dasatinib (if depicted in the respective publication). /: no information available, **B5D**: five consecutive days bid dosing followed by two nontreatment days, **B7D**: seven consecutive days bid dosing, **bid**: twice a day, **md**: multiple dose, **n**: number of participants, **po**: peroral, **Q5D**: five consecutive days once daily dosing followed by two nontreatment days, **qd**: once a day, **sd**: single dose, **tab**: tablet.

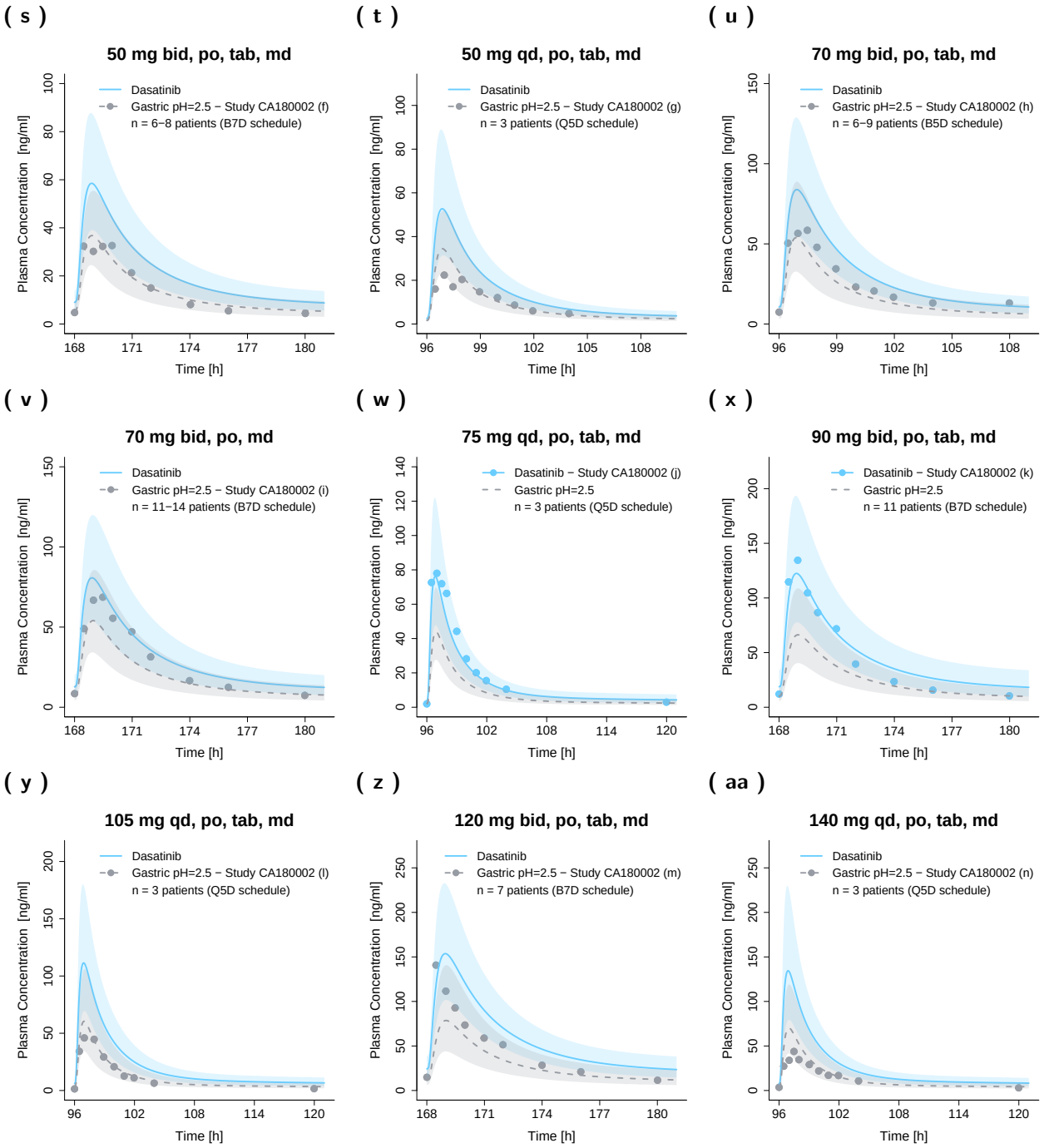

Figure S3: (*continued*) **Predicted and observed dasatinib plasma concentration–time profiles in cancer patients on a linear scale.** Solid and dashed lines show predicted geometric mean concentration–time profiles with gastric pH of 2.0 and 2.5, respectively, with ribbons illustrating the corresponding geometric standard deviation of the population simulations (n=100). Points demonstrate the mean observed data with the corresponding standard deviation of dasatinib (if depicted in the respective publication). /: no information available, **B5D**: five consecutive days bid dosing followed by two nontreatment days, **B7D**: seven consecutive days bid dosing, **bid**: twice a day, **md**: multiple dose, **n**: number of participants, **po**: peroral, **Q5D**: five consecutive days once daily dosing followed by two nontreatment days, **qd**: once a day, **sd**: single dose, **tab**: tablet.

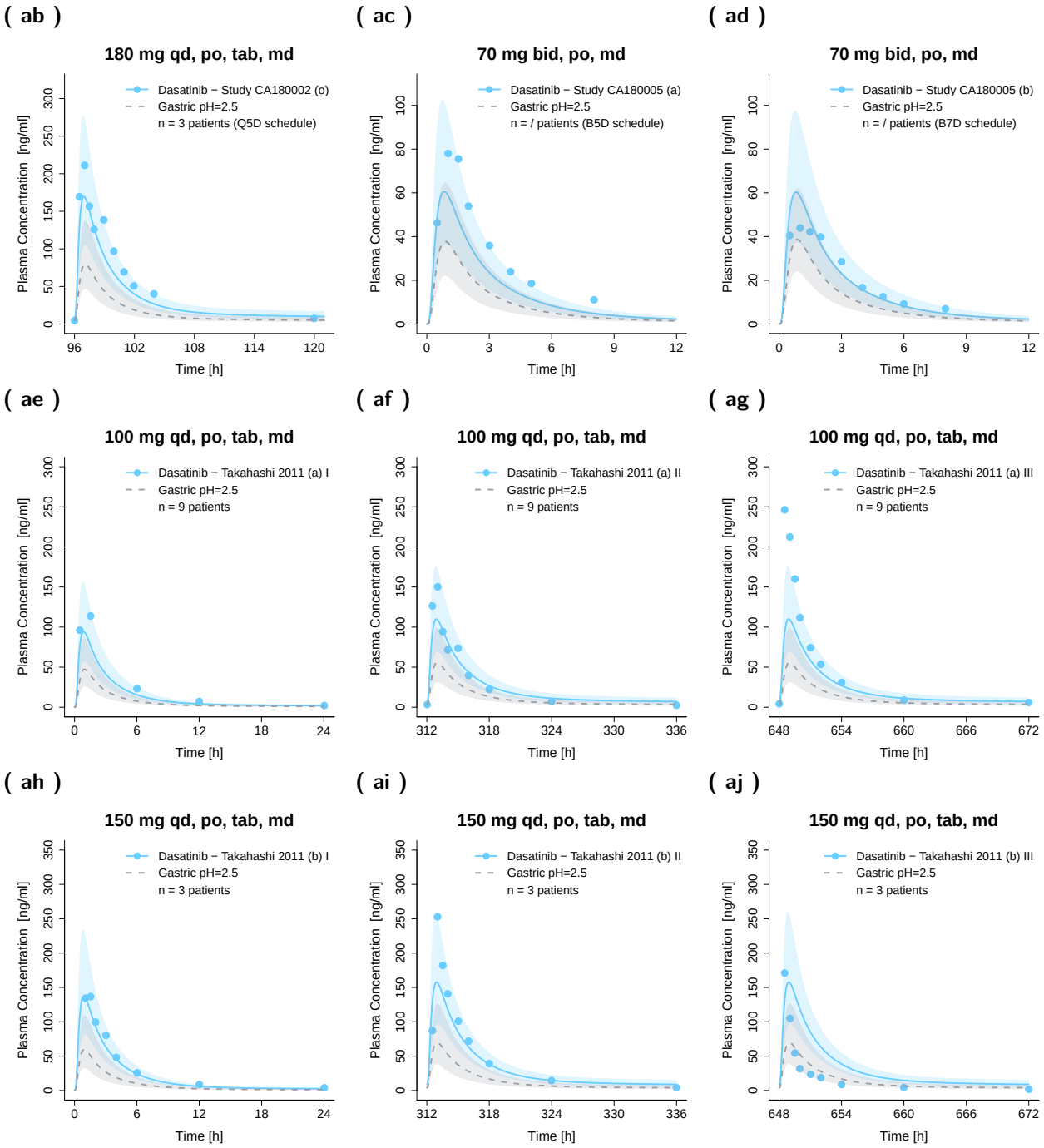

Figure S3: (*continued*) **Predicted and observed dasatinib plasma concentration–time profiles in cancer patients on a linear scale.** Solid and dashed lines show predicted geometric mean concentration–time profiles with gastric pH of 2.0 and 2.5, respectively, with ribbons illustrating the corresponding geometric standard deviation of the population simulations (n=100). Points demonstrate the mean observed data with the corresponding standard deviation of dasatinib (if depicted in the respective publication). /: no information available, **B5D**: five consecutive days bid dosing followed by two nontreatment days, **B7D**: seven consecutive days bid dosing, **bid**: twice a day, **md**: multiple dose, **n**: number of participants, **po**: peroral, **Q5D**: five consecutive days once daily dosing followed by two nontreatment days, **qd**: once a day, **sd**: single dose, **tab**: tablet.

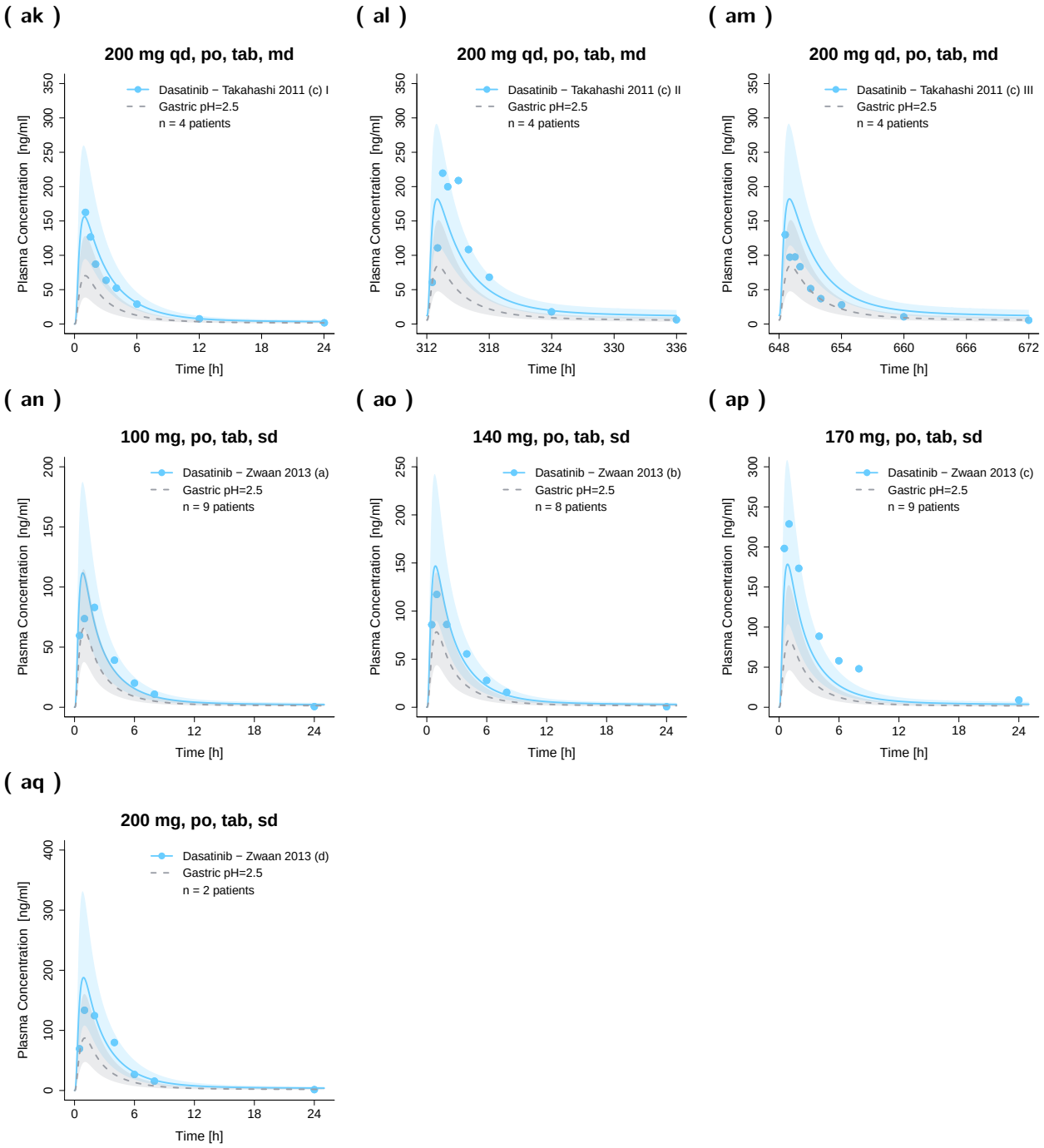

Figure S3: (*continued*) **Predicted and observed dasatinib plasma concentration–time profiles in cancer patients on a linear scale.** Solid and dashed lines show predicted geometric mean concentration–time profiles with gastric pH of 2.0 and 2.5, respectively, with ribbons illustrating the corresponding geometric standard deviation of the population simulations (n=100). Points demonstrate the mean observed data with the corresponding standard deviation of dasatinib (if depicted in the respective publication). /: no information available, **B5D**: five consecutive days bid dosing followed by two nontreatment days, **B7D**: seven consecutive days bid dosing, **bid**: twice a day, **md**: multiple dose, **n**: number of participants, **po**: peroral, **Q5D**: five consecutive days once daily dosing followed by two nontreatment days, **qd**: once a day, **sd**: single dose, **tab**: tablet.

S2.2.2 Plasma Profiles (Semilogarithmic Scale)

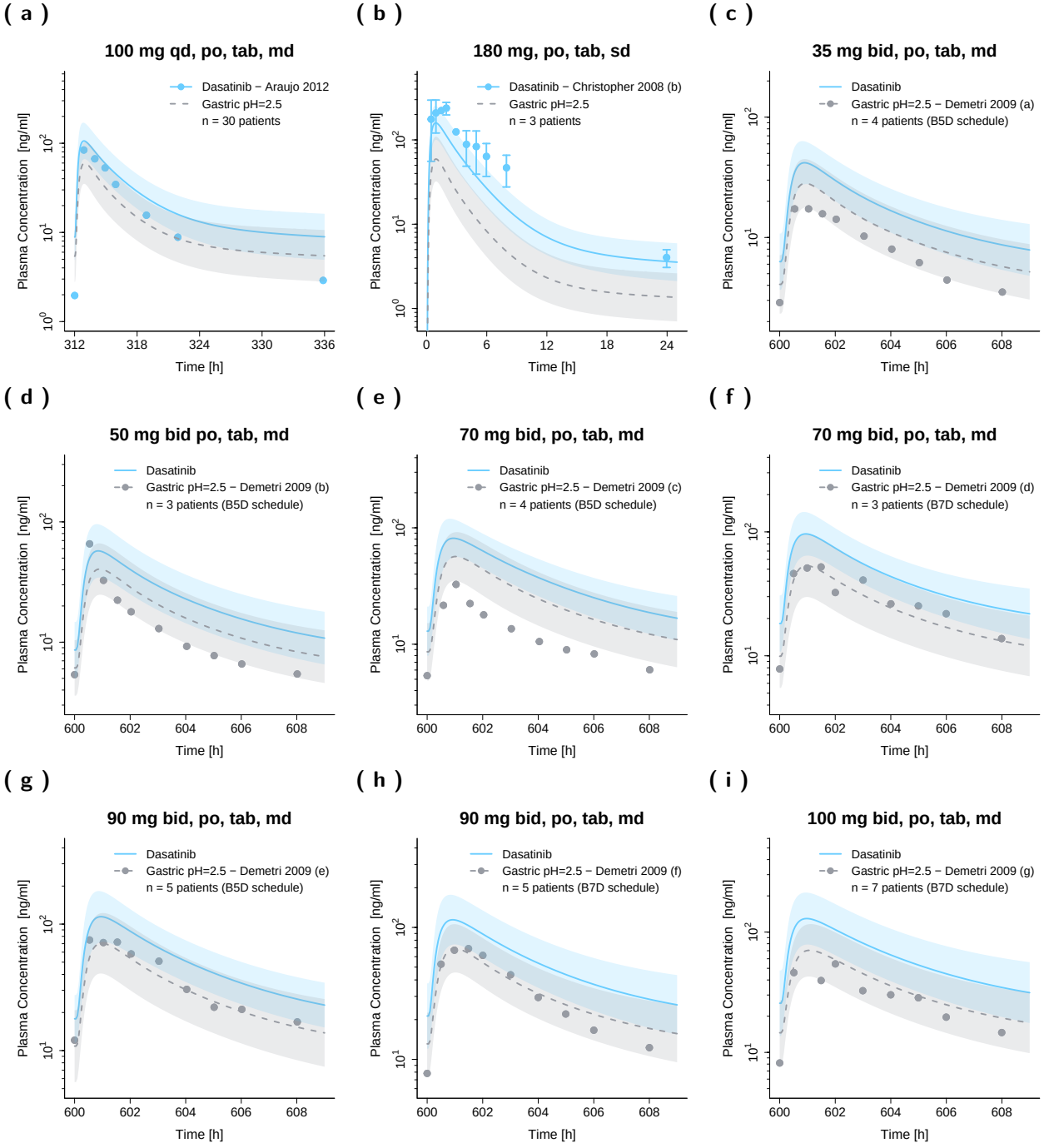

Figure S4: Predicted and observed dasatinib plasma concentration–time profiles in cancer patients on a semilogarithmic scale. Solid and dashed lines show predicted geometric mean concentration–time profiles with gastric pH of 2.0 and 2.5, respectively, with ribbons illustrating the corresponding geometric standard deviation of the population simulations (n=100). Points demonstrate the mean observed data with the corresponding standard deviation of dasatinib (if depicted in the respective publication). /: no information available, **B5D**: five consecutive days bid dosing followed by two nontreatment days, **B7D**: seven consecutive days bid dosing, **bid**: twice a day, **md**: multiple dose, **n**: number of participants, **po**: peroral, **Q5D**: five consecutive days once daily dosing followed by two nontreatment days, **qd**: once a day, **sd**: single dose, **tab**: tablet.

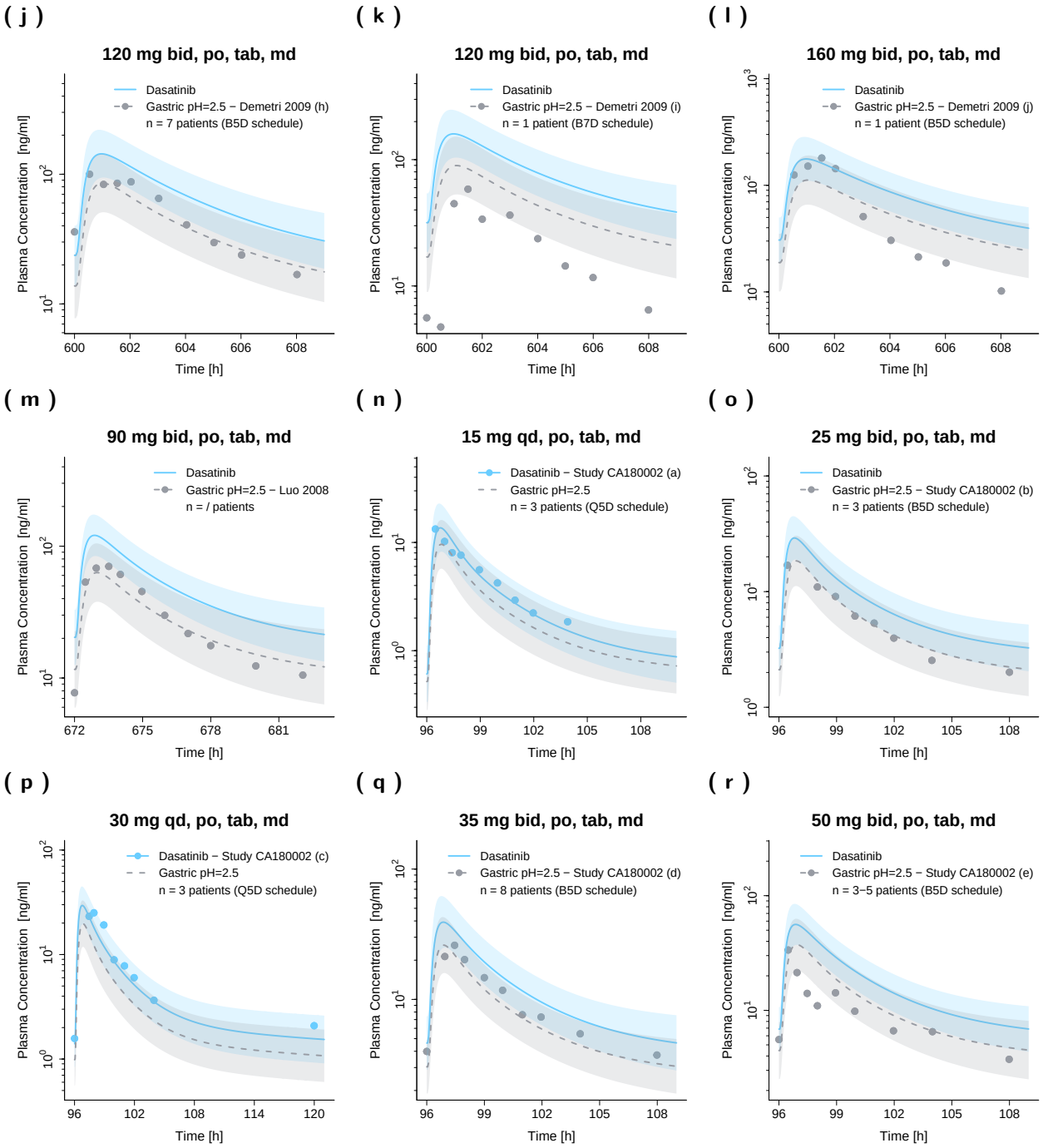

Figure S4: (*continued*) **Predicted and observed dasatinib plasma concentration–time profiles in cancer patients on a semilogarithmic scale.** Solid and dashed lines show predicted geometric mean concentration–time profiles with gastric pH of 2.0 and 2.5, respectively, with ribbons illustrating the corresponding geometric standard deviation of the population simulations (n=100). Points demonstrate the mean observed data with the corresponding standard deviation of dasatinib (if depicted in the respective publication). /: no information available, **B5D**: five consecutive days bid dosing followed by two nontreatment days, **B7D**: seven consecutive days bid dosing, **bid**: twice a day, **md**: multiple dose, **n**: number of participants, **po**: peroral, **Q5D**: five consecutive days once daily dosing followed by two nontreatment days, **qd**: once a day, **sd**: single dose, **tab**: tablet.

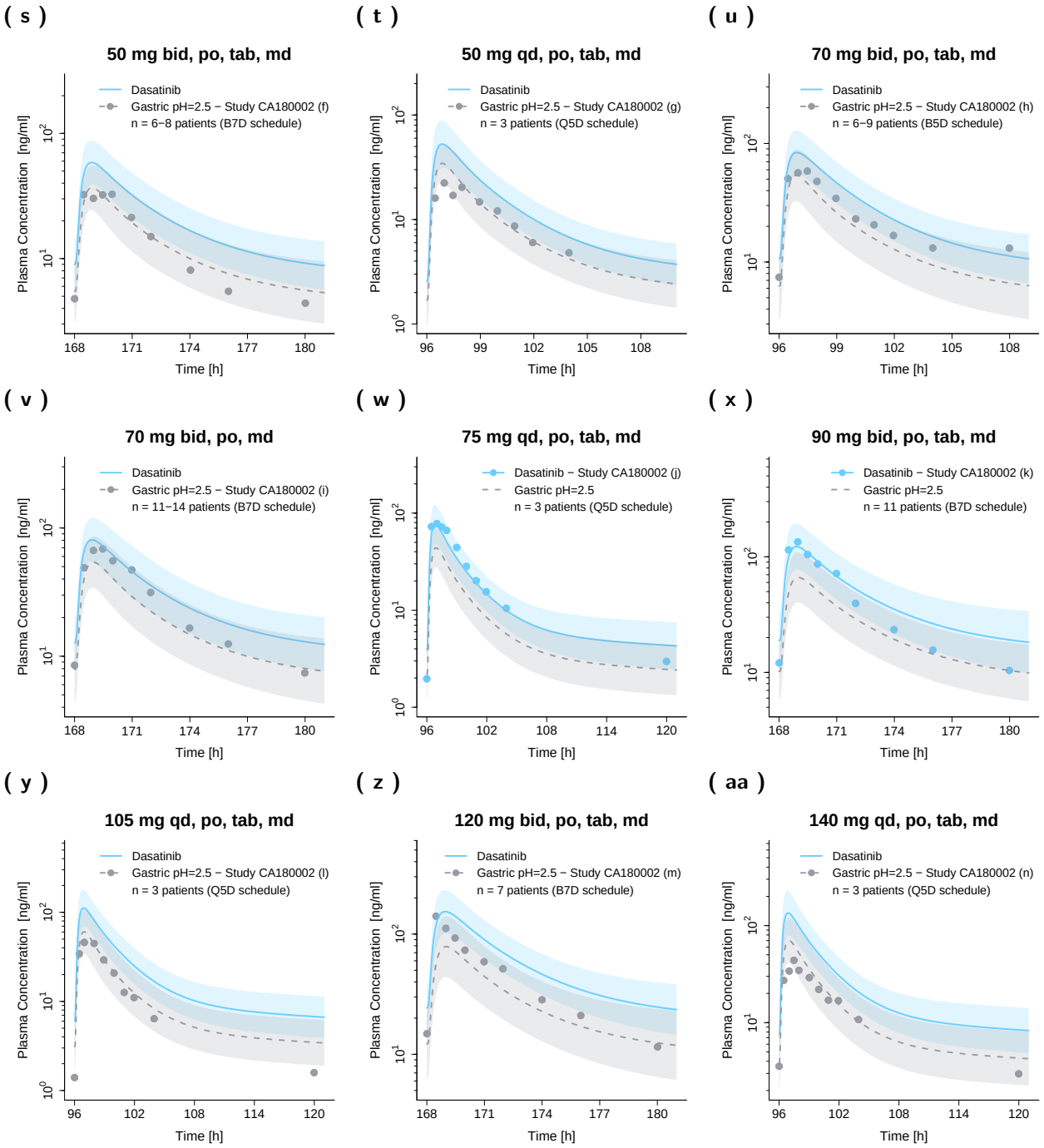

Figure S4: (*continued*) **Predicted and observed dasatinib plasma concentration–time profiles in cancer patients on a semilogarithmic scale.** Solid and dashed lines show predicted geometric mean concentration–time profiles with gastric pH of 2.0 and 2.5, respectively, with ribbons illustrating the corresponding geometric standard deviation of the population simulations (n=100). Points demonstrate the mean observed data with the corresponding standard deviation of dasatinib (if depicted in the respective publication). /: no information available, **B5D**: five consecutive days bid dosing followed by two nontreatment days, **B7D**: seven consecutive days bid dosing, **bid**: twice a day, **md**: multiple dose, **n**: number of participants, **po**: peroral, **Q5D**: five consecutive days once daily dosing followed by two nontreatment days, **qd**: once a day, **sd**: single dose, **tab**: tablet.

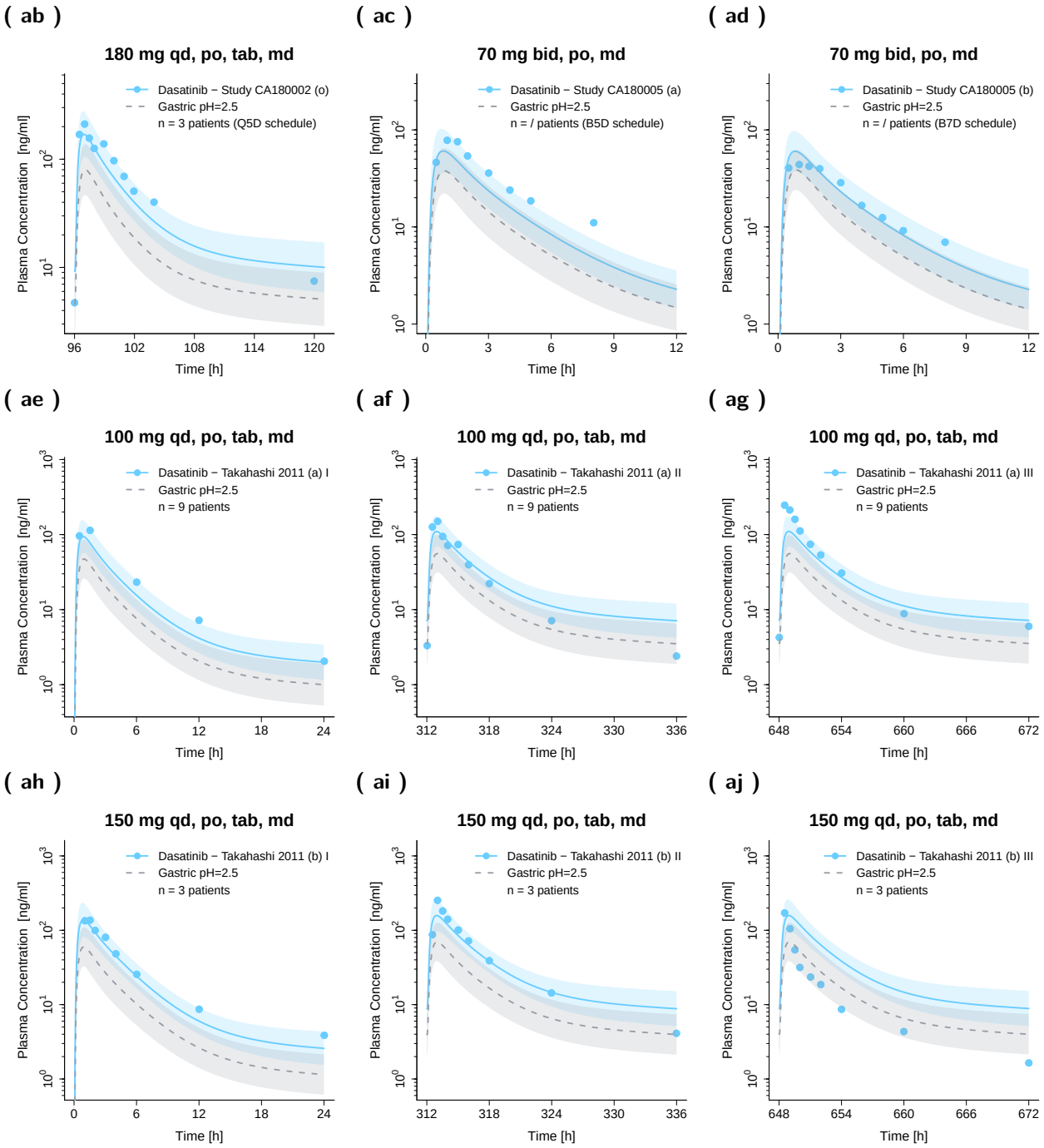

Figure S4: (*continued*) **Predicted and observed dasatinib plasma concentration–time profiles in cancer patients on a semilogarithmic scale.** Solid and dashed lines show predicted geometric mean concentration–time profiles with gastric pH of 2.0 and 2.5, respectively, with ribbons illustrating the corresponding geometric standard deviation of the population simulations (n=100). Points demonstrate the mean observed data with the corresponding standard deviation of dasatinib (if depicted in the respective publication). /: no information available, **B5D**: five consecutive days bid dosing followed by two nontreatment days, **B7D**: seven consecutive days bid dosing, **bid**: twice a day, **md**: multiple dose, **n**: number of participants, **po**: peroral, **Q5D**: five consecutive days once daily dosing followed by two nontreatment days, **qd**: once a day, **sd**: single dose, **tab**: tablet.

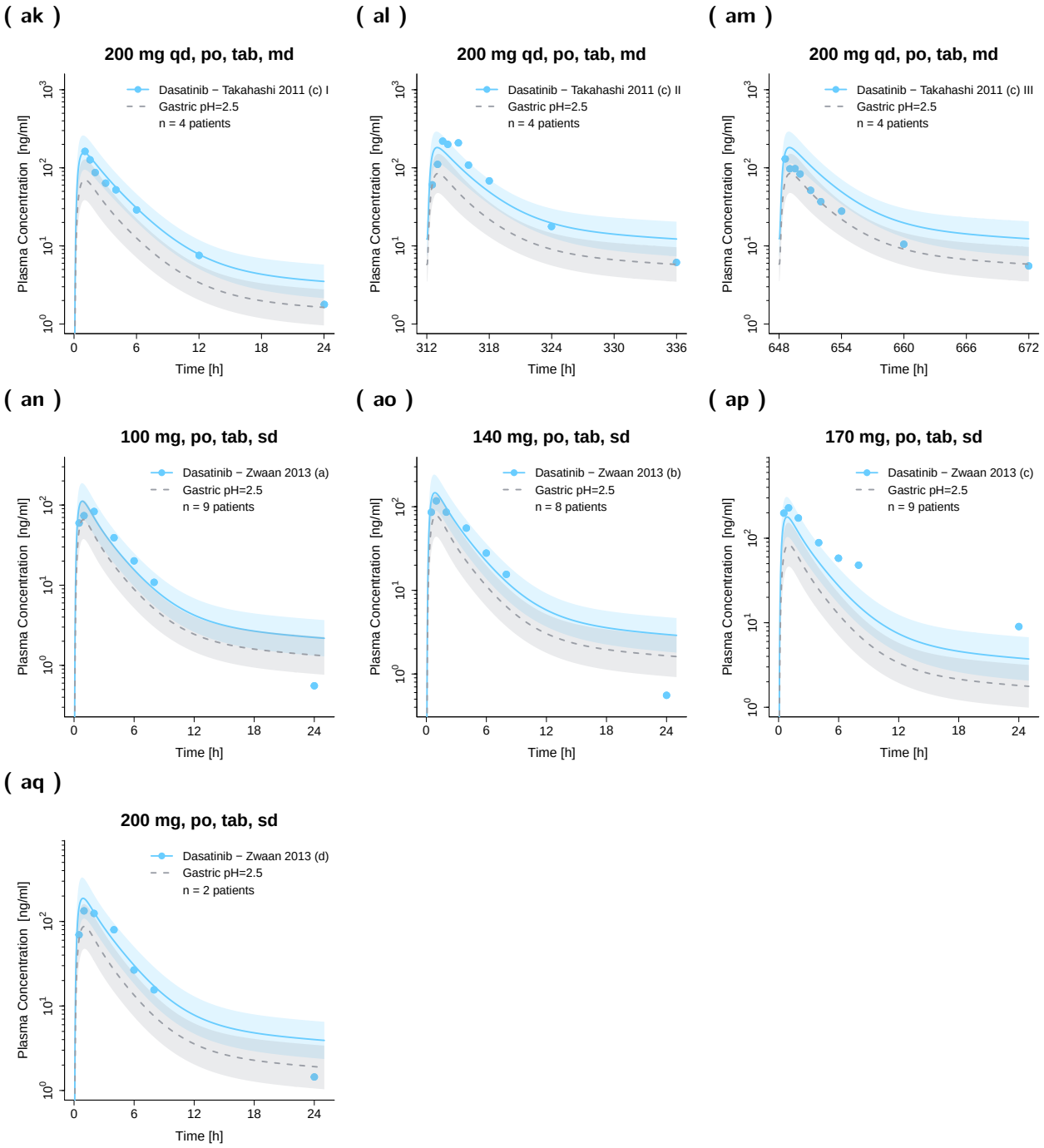

Figure S4: (*continued*) **Predicted and observed dasatinib plasma concentration–time profiles in cancer patients on a semilogarithmic scale.** Solid and dashed lines show predicted geometric mean concentration–time profiles with gastric pH of 2.0 and 2.5, respectively, with ribbons illustrating the corresponding geometric standard deviation of the population simulations (n=100). Points demonstrate the mean observed data with the corresponding standard deviation of dasatinib (if depicted in the respective publication). /: no information available, **B5D**: five consecutive days bid dosing followed by two nontreatment days, **B7D**: seven consecutive days bid dosing, **bid**: twice a day, **md**: multiple dose, **n**: number of participants, **po**: peroral, **Q5D**: five consecutive days once daily dosing followed by two nontreatment days, **qd**: once a day, **sd**: single dose, **tab**: tablet.

S2.2.3 Goodness-of-fit Plots

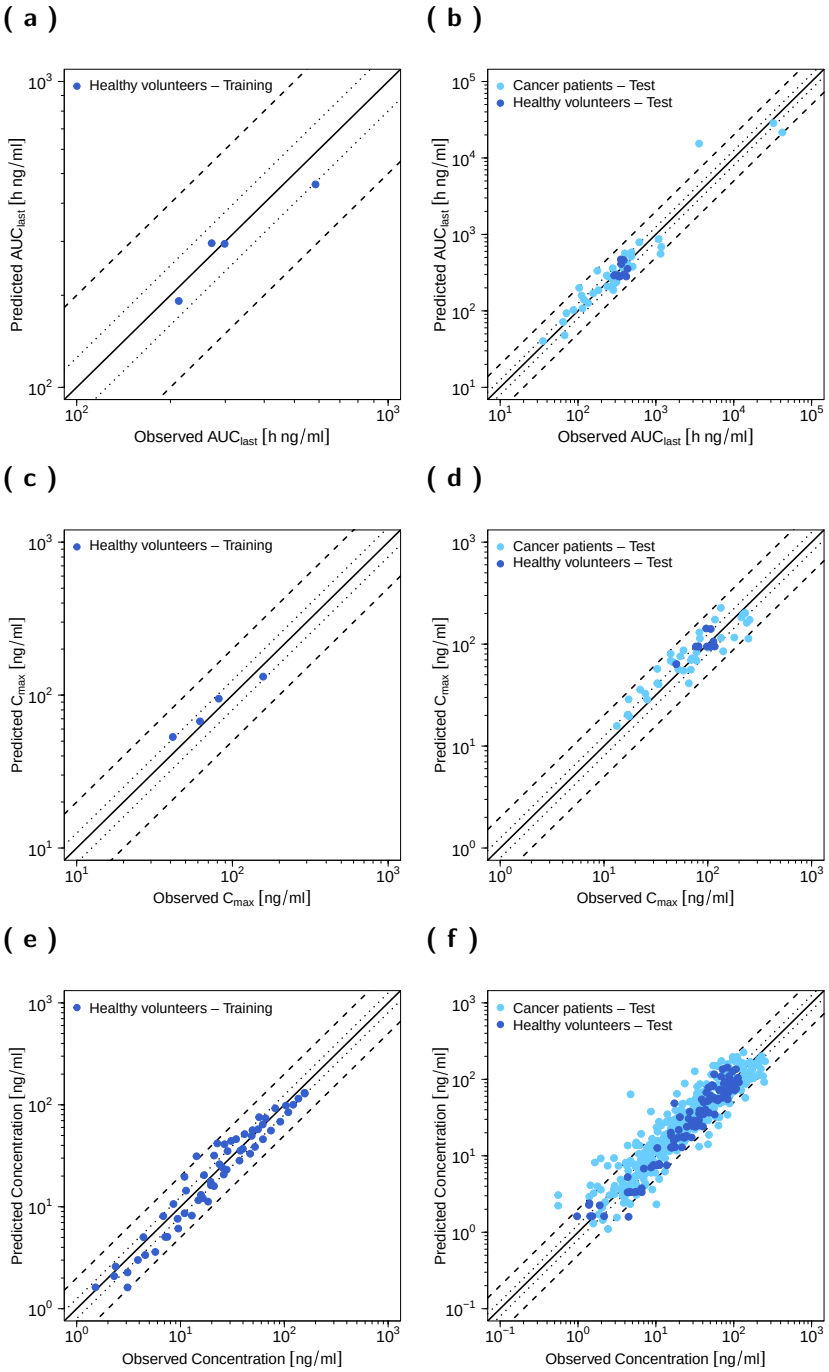

Figure S5: Goodness-of-fit plots of predicted versus observed AUC_{last} (a–b), C_{max} (c–d) and plasma concentrations (e–f) of the training (first column) and test dataset (second column). Solid lines mark the lines of identity, dotted lines indicate 1.25-fold and dashed lines two-fold deviation. **AUC_{last}**: areas under the plasma concentration–time curves from the first to the last time point of measurement, **C_{max}**: maximum plasma concentration.

S2.2.4 Residual Plot

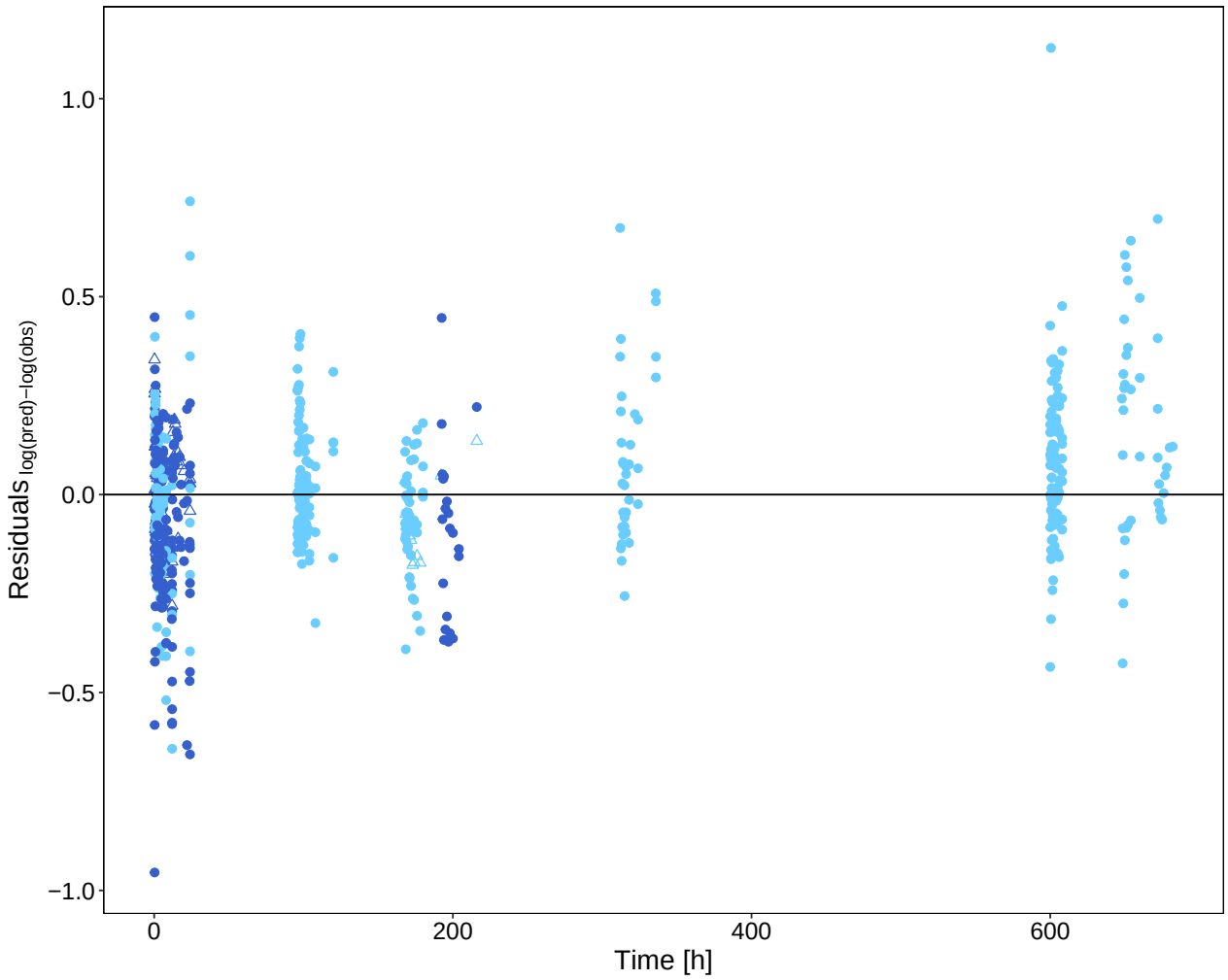

Figure S6: Residuals versus time. Blue and light blue symbols represent residuals from healthy volunteers and cancer patients, respectively. Triangles indicate residuals from the training dataset, while points indicate residuals from the test dataset. **Obs**: observed concentration, **pred**: predicted concentration.

S2.3 Quantitative PBPK Model Evaluation

S2.3.1 Geometric Mean Fold Error (GMFE)

Table S5: Geometric Mean Fold Error (GMFE) of C_{max} and AUC_{last} Predictions.

		$\mathbf{C_{max}}$			$\mathbf{AUC_{last}}$			
Administration	Compound	Pred $\left[\frac{ng}{ml}\right]$	Obs $\left[\frac{ng}{ml}\right]$	Pred/Obs	Pred $\left[\frac{ng \cdot h}{ml}\right]$	Obs $\left[\frac{ng \cdot h}{ml}\right]$	Pred/Obs	Reference
140 mg, po, tab, sd	Dasatinib	132.01	157.54	0.84	460.68	584.68	0.79	Bioequivalence study [13]
100 mg, po, sol, sd	Dasatinib	142.39	96.56	1.47	470.88	355.02	1.33	Christopher 2008 (a) [7]
50 mg, po, tab, bid, md	Dasatinib	53.24	41.43	1.29	295.99	271.31	1.09	Eley 2009 (control) [50]
100 mg, po, tab, sd	Dasatinib	94.78	81.72	1.16	294.52	298.60	0.99	Furlong 2012 [14]
100 mg, po, tab, sd	Dasatinib	140.72	106.81	1.32	461.41	387.37	1.19	Yago 2014 (control) [51]
100 mg, po, tab, sd	Dasatinib	94.78	81.31	1.17	292.05	323.65	0.90	Study CA180009 (fasted state (a)) [6]
100 mg, po, tab, sd	Dasatinib	63.76	49.78	1.28	410.28	357.61	1.15	Study CA180009 (with high–fat meal (b)) [6]
100 mg, po, tab, sd	Dasatinib	94.78	98.08	0.97	298.20	387.83	0.77	Study CA180009 (with light–fat meal (c)) [6]
100 mg, po, tab, sd	Dasatinib	94.78	76.82	1.23	293.25	301.65	0.97	Study CA180016 [6]
100 mg, po, tab, sd	Dasatinib	94.84	80.93	1.17	290.68	291.31	1.00	Study CA180032 (control) [6]
70 mg, po, tab, sd	Dasatinib	67.32	61.96	1.09	191.56	212.69	0.90	Vaidhyanathan 2018 (a) [8]
100 mg, po, PFOS, sd	Dasatinib	94.78	106.27	0.89	282.00	334.05	0.84	Vaidhyanathan 2018 (b) [8]
100 mg, po, dispersed tab, sd	Dasatinib	94.78	107.35	0.88	281.99	345.96	0.82	Vaidhyanathan 2018 (c) [8]
100 mg, po, tab, sd	Dasatinib	94.78	116.56	0.81	281.44	416.37	0.68	Vaidhyanathan 2018 (d) [8]
100 mg, po, tab, sd	Dasatinib	106.04	113.27	0.94	354.01	432.84	0.82	Vargas 2016 [9]
100 mg, po, tab, qd, md	Dasatinib	113.57	84.00	1.35	565.38	400.19	1.41	Araujo 2012 [15]
180 mg, po, tab, sd	Dasatinib	161.85	237.86	0.68	557.79	1149.40	0.49	Christopher 2008 (b) [7]
35 mg, po, tab, bid, md (B5D)	Dasatinib	28.74	17.28	1.66	93.48	71.05	1.32	Demetri 2009 (a) [16]
50 mg, po, tab, bid, md (B5D)	Dasatinib	41.23	65.65	0.63	139.03	120.09	1.16	Demetri 2009 (b) [16]
70 mg, po, tab, bid, md (B5D)	Dasatinib	57.16	32.64	1.75	199.85	103.69	1.93	Demetri 2009 (c) [16]
70 mg, po, tab, bid, md (B7D)	Dasatinib	56.47	52.12	1.08	207.76	238.01	0.87	Demetri 2009 (d) [16]
90 mg, po, tab, bid, md (B5D)	Dasatinib	72.10	74.88	0.96	258.15	307.42	0.84	Demetri 2009 (e) [16]
90 mg, po, tab, bid, md (B7D))	Dasatinib	69.87	69.03	1.01	263.07	273.55	0.96	Demetri 2009 (f) [16]
100 mg, po, tab, bid, md (B7D)	Dasatinib	75.90	54.40	1.40	284.12	240.30	1.18	Demetri 2009 (g) [16]
120 mg, po, tab, bid, md (B5D)	Dasatinib	92.46	100.07	0.92	339.75	396.39	0.86	Demetri 2009 (h) [16]
120 mg, po, tab, bid, md (B7D)	Dasatinib	86.73	58.42	1.48	334.03	177.28	1.88	Demetri 2009 (i) [16]
160 mg, po, tab, bid, md (B5D)	Dasatinib	116.02	180.29	0.64	413.91	433.80	0.95	Demetri 2009 (j) [16]
20 mg, po, tab, sd	Dasatinib	19.57	17.48	1.12	47.93	67.26	0.71	Johnson 2010 (control) [52]
90 mg, po, tab, bid, md	Dasatinib	72.47	70.28	1.03	306.38	301.74	1.02	Luo 2008 [10]

(continued)

Table S5: Geometric Mean Fold Error (GMFE) of C_{max} and AUC_{last} Predictions *(continued)*.

		$\mathbf{C_{max}}$			$\mathbf{AUC_{last}}$			
Administration	Compound	Pred $\left[\frac{ng}{ml}\right]$	Obs $\left[\frac{ng}{ml}\right]$	Pred/Obs	Pred $\left[\frac{ng \cdot h}{ml}\right]$	Obs $\left[\frac{ng \cdot h}{ml}\right]$	Pred/Obs	Reference
15 mg, po, tab, qd, md (Q5D)	Dasatinib	15.77	13.30	1.19	40.22	35.50	1.13	Study CA180002 (a) [6]
25 mg, po, tab, bid, md (B5D)	Dasatinib	20.31	16.92	1.20	71.56	64.47	1.11	Study CA180002 (b) [6]
30 mg, po, tab, qd, md (Q5D)	Dasatinib	32.63	25.09	1.30	127.07	134.72	0.94	Study CA180002 (c) [6]
35 mg, po, tab, bid, md (B5D)	Dasatinib	28.55	26.02	1.10	107.80	114.35	0.94	Study CA180002 (d) [6]
50 mg, po, tab, bid, md (B5D)	Dasatinib	40.40	33.59	1.20	158.70	111.15	1.43	Study CA180002 (e) [6]
50 mg, po, tab, bid, md (B7D)	Dasatinib	41.34	32.63	1.27	169.28	156.54	1.08	Study CA180002 (f) [6]
50 mg, po, tab, qd, md (Q5D)	Dasatinib	35.72	22.36	1.60	102.44	87.51	1.17	Study CA180002 (g) [6]
70 mg, po, tab, bid, md (B5D)	Dasatinib	54.84	58.47	0.94	223.45	287.82	0.78	Study CA180002 (h) [6]
70 mg, po, tab, bid, md (B7D)	Dasatinib	56.15	68.66	0.82	237.56	311.15	0.76	Study CA180002 (i) [6]
75 mg, po, tab, qd, md (Q5D)	Dasatinib	83.54	78.00	1.07	363.20	380.49	0.95	Study CA180002 (j) [6]
90 mg, po, tab, bid, md (B7D)	Dasatinib	115.01	134.50	0.86	512.27	484.38	1.06	Study CA180002 (k) [6]
105 mg, po, tab, qd, md (Q5D)	Dasatinib	66.62	45.93	1.45	290.29	234.29	1.24	Study CA180002 (l) [6]
120 mg, po, tab, bid, md (B7D)	Dasatinib	85.07	140.79	0.60	378.38	503.90	0.75	Study CA180002 (m) [6]
140 mg, po, tab, qd, md (Q5D)	Dasatinib	80.35	43.84	1.83	360.80	278.94	1.29	Study CA180002 (n) [6]
180 mg, po, tab, qd, md (Q5D)	Dasatinib	182.78	211.15	0.87	868.30	1086.35	0.80	Study CA180002 (o) [6]
70 mg, po, tab, bid, md (B5D)	Dasatinib	68.62	78.02	0.88	187.28	283.48	0.66	Study CA180005 (a) [6]
70 mg, po, tab, bid, md (B7D)	Dasatinib	68.62	43.92	1.56	186.53	182.88	1.02	Study CA180005 (b) [6]
100 mg, po, tab, qd, md	Dasatinib	113.21	246.31	0.46	15399.80	3590.79	4.29	Takahashi 2011 (a) [17]
150 mg, po, tab, qd, md	Dasatinib	173.08	252.88	0.68	21560.86	42110.33	0.51	Takahashi 2011 (b) [17]
200 mg, po, tab, qd, md	Dasatinib	196.19	219.58	0.89	28503.51	32382.36	0.88	Takahashi 2011 (c) [17]
100 mg, po, tab, qd, sd	Dasatinib	130.21	83.05	1.57	419.24	370.40	1.13	Zwaan 2013 (a) [12]
140 mg, po, tab, qd, sd	Dasatinib	173.94	117.30	1.48	583.41	485.17	1.20	Zwaan 2013 (b) [12]
170 mg, po, tab, qd, sd	Dasatinib	202.39	228.72	0.88	688.11	1174.63	0.59	Zwaan 2013 (c) [12]
200 mg, po, tab, qd, sd	Dasatinib	226.89	133.54	1.70	789.00	613.16	1.29	Zwaan 2013 (d) [12]
		GMFE: 1.29 (1.01–2.18)			**GMFE: 1.27 (1.00–4.29)**			
		GMFE ≤ 2: 52/53			**GMFE ≤ 2: 51/53**			

AUC_{last}: area under the plasma concentration–time curve from the first to the last time point of measurement, **B5D**: five consecutive days bid dosing followed by two nontreatment days, **B7D**: continuous bid dosing, **bid**: twice a day, **C_{max}**: maximum plasma concentration, **DFI**, drug–food interaction, **md**: multiple dose, **Obs**: observed, **PFOS**: powder for oral suspension, **po**: peroral, **Pred**: predicted, **Q5D**: five consecutive days once daily dosing followed by two nontreatment days, **qd**: once a day, **sd**: single dose, **sol**: solution, **tab**: tablet

S2.3.2 Mean Relative Deviation (MRD)

Table S6: Mean relative deviation (MRD) values of dasatinib plasma concentration predictions.

Administration	Compound	Health Status	MRD	Reference
140 mg, po, tab, sd	Dasatinib	Healthy	1.36	Bioequivalence study [13]
100 mg, po, sol, sd	Dasatinib	Healthy	1.54	Christopher 2008 (a) [7]
50 mg, po, tab, bid, md	Dasatinib	Healthy	1.43	Eley 2009 (control) [50]
100 mg, po, tab, sd	Dasatinib	Healthy	1.18	Furlong 2012 [14]
100 mg, po, tab, sd	Dasatinib	Healthy	1.37	Yago 2014 (control) [51]
100 mg, po, tab, sd	Dasatinib	Healthy	1.29	Study CA180009 (at fasted state (a)) [6]
100 mg, po, tab, sd	Dasatinib	Healthy	1.34	Study CA180009 (with high–fat meal (b)) [6]
100 mg, po, tab, sd	Dasatinib	Healthy	1.15	Study CA180009 (with light–fat meal (c)) [6]
100 mg, po, tab, sd	Dasatinib	Healthy	1.25	Study CA180016 [6]
100 mg, po, tab, sd	Dasatinib	Healthy	1.28	Study CA180032 (control) [6]
70 mg, po, tab, sd	Dasatinib	Healthy	1.31	Vaidhyanathan 2018 (a) [8]
100 mg, po, PFOS, sd	Dasatinib	Healthy	1.26	Vaidhyanathan 2018 (b) [8]
100 mg, po, dispersed tab, sd	Dasatinib	Healthy	1.32	Vaidhyanathan 2018 (c) [8]
100 mg, po, tab, sd	Dasatinib	Healthy	1.60	Vaidhyanathan 2018 (d) [8]
100 mg, po, tab, sd	Dasatinib	Healthy	1.63	Vargas 2016 [9]
100 mg, po, tab, qd, md	Dasatinib	Cancer	2.07	Araujo 2012 [15]
180 mg, po, tab, sd	Dasatinib	Cancer	2.01	Christopher 2008 (b) [7]
35 mg, po, tab, bid, md (B5D)	Dasatinib	Cancer	1.35	Demetri 2009 (a) [16]
50 mg, po, tab, bid, md (B5D)	Dasatinib	Cancer	1.49	Demetri 2009 (b) [16]
70 mg, po, tab, bid, md (B5D)	Dasatinib	Cancer	1.91	Demetri 2009 (c) [16]
70 mg, po, tab, bid, md (B7D)	Dasatinib	Cancer	1.26	Demetri 2009 (d) [16]
90 mg, po, tab, bid, md (B5D)	Dasatinib	Cancer	1.21	Demetri 2009 (e) [16]
90 mg, po, tab, bid, md (B7D))	Dasatinib	Cancer	1.19	Demetri 2009 (f) [16]
100 mg, po, tab, bid, md (B7D)	Dasatinib	Cancer	1.30	Demetri 2009 (g) [16]
120 mg, po, tab, bid, md (B5D)	Dasatinib	Cancer	1.44	Demetri 2009 (h) [16]
120 mg, po, tab, bid, md (B7D)	Dasatinib	Cancer	2.89	Demetri 2009 (i) [16]
160 mg, po, tab, bid, md (B5D)	Dasatinib	Cancer	1.66	Demetri 2009 (j) [16]
20 mg, po, tab, sd	Dasatinib	Cancer	1.64	Johnson 2010 (control) [52]
90 mg, po, tab, bid, md	Dasatinib	Cancer	1.24	Luo 2008 [10]
15 mg, po, tab, qd, md (Q5D)	Dasatinib	Cancer	1.21	Study CA180002 (a) [6]
25 mg, po, tab, bid, md (B5D)	Dasatinib	Cancer	1.13	Study CA180002 (b) [6]
30 mg, po, tab, qd, md (Q5D)	Dasatinib	Cancer	1.24	Study CA180002 (c) [6]
35 mg, po, tab, bid, md (B5D)	Dasatinib	Cancer	1.22	Study CA180002 (d) [6]
50 mg, po, tab, bid, md (B5D)	Dasatinib	Cancer	1.67	Study CA180002 (e) [6]
50 mg, po, tab, bid, md (B7D)	Dasatinib	Cancer	1.19	Study CA180002 (f) [6]
50 mg, po, tab, qd, md (Q5D)	Dasatinib	Cancer	1.33	Study CA180002 (g) [6]
70 mg, po, tab, bid, md (B5D)	Dasatinib	Cancer	1.37	Study CA180002 (h) [6]
70 mg, po, tab, bid, md (B7D)	Dasatinib	Cancer	1.30	Study CA180002 (i) [6]
75 mg, po, tab, qd, md (Q5D)	Dasatinib	Cancer	1.25	Study CA180002 (j) [6]
90 mg, po, tab, bid, md (B7D)	Dasatinib	Cancer	1.28	Study CA180002 (k) [6]
105 mg, po, tab, qd, md (Q5D)	Dasatinib	Cancer	1.47	Study CA180002 (l) [6]
120 mg, po, tab, bid, md (B7D)	Dasatinib	Cancer	1.42	Study CA180002 (m) [6]
140 mg, po, tab, qd, md (Q5D)	Dasatinib	Cancer	1.53	Study CA180002 (n) [6]
180 mg, po, tab, qd, md (Q5D)	Dasatinib	Cancer	1.34	Study CA180002 (o) [6]
70 mg, po, tab, bid, md (B5D)	Dasatinib	Cancer	1.89	Study CA180005 (a) [6]
70 mg, po, tab, bid, md (B7D)	Dasatinib	Cancer	1.36	Study CA180005 (b) [6]
100 mg, po, tab, qd, md	Dasatinib	Cancer	1.58	Takahashi 2011 (a) [17]
150 mg, po, tab, qd, md	Dasatinib	Cancer	2.08	Takahashi 2011 (b) [17]
200 mg, po, tab, qd, md	Dasatinib	Cancer	1.72	Takahashi 2011 (c) [17]

(continued)

Table S6: Mean relative deviation (MRD) values of dasatinib plasma concentration predictions *(continued)*.

Study	Compound	Health Status	MRD	Reference
100 mg, po, tab, qd, sd	Dasatinib	Cancer	1.84	Zwaan 2013 (a) [12]
140 mg, po, tab, qd, sd	Dasatinib	Cancer	2.00	Zwaan 2013 (b) [12]
170 mg, po, tab, qd, sd	Dasatinib	Cancer	1.78	Zwaan 2013 (c) [12]
200 mg, po, tab, qd, sd	Dasatinib	Cancer	1.81	Zwaan 2013 (d) [12]
Overall MRD: 1.54 (1.13–2.89)				
49/53 MRD ≤ 2				

B5D: five consecutive days bid dosing followed by two nontreatment days, **B7D**: continuous bid dosing, **bid**: twice a day, **DFI**: drug–food interaction, **md**: multiple dose, **PFOS**: powder for oral suspension, **po**: peroral, **Q5D**: five consecutive days once daily dosing followed by two nontreatment days, **qd**: once a day, **sd**: single dose, **sol**: solution, **tab**: tablet

S2.4 Local Sensitivity Analysis

S2.4.1 Mathematical Implementation

A sensitivity analysis was conducted by calculating the impact of single parameter changes (local sensitivity analysis) on the predicted AUC_{inf}. Here, the relative change of AUC_{inf} at steady-state after peroral administration of 100 mg dasatinib daily to the relative variation of model input parameters was calculated according to Equation S1. Parameters were included in the sensitivity analysis, if they were optimized (I), assumed to affect AUC_{inf} (II) or might have a strong impact due to their use in the calculation of permeabilities or partition coefficients (III). A relative perturbation of 1000% (variation range 10.0, maximum number of 9 steps) was utilized. Parameters were considered sensitive if their sensitivity value was equal or greater than |0.5|. For instance, a sensitivity of +0.5 implies that a 100% increase of the examined parameter value leads to a 50% increase of the simulated AUC_{inf}.

$$S = \frac{\Delta AUC_{inf}}{\Delta p} \cdot \frac{p}{AUC_{inf}} \tag{S1}$$

S = sensitivity of the AUC_{inf} to the examined model parameter, ΔAUC_{inf} = change of the AUC_{inf}, AUC_{inf} = simulated AUC_{inf} with the original parameter value, p = original model parameter value, Δp = variation of the model parameter value

S2.4.2 Results of the Sensitivity Analysis

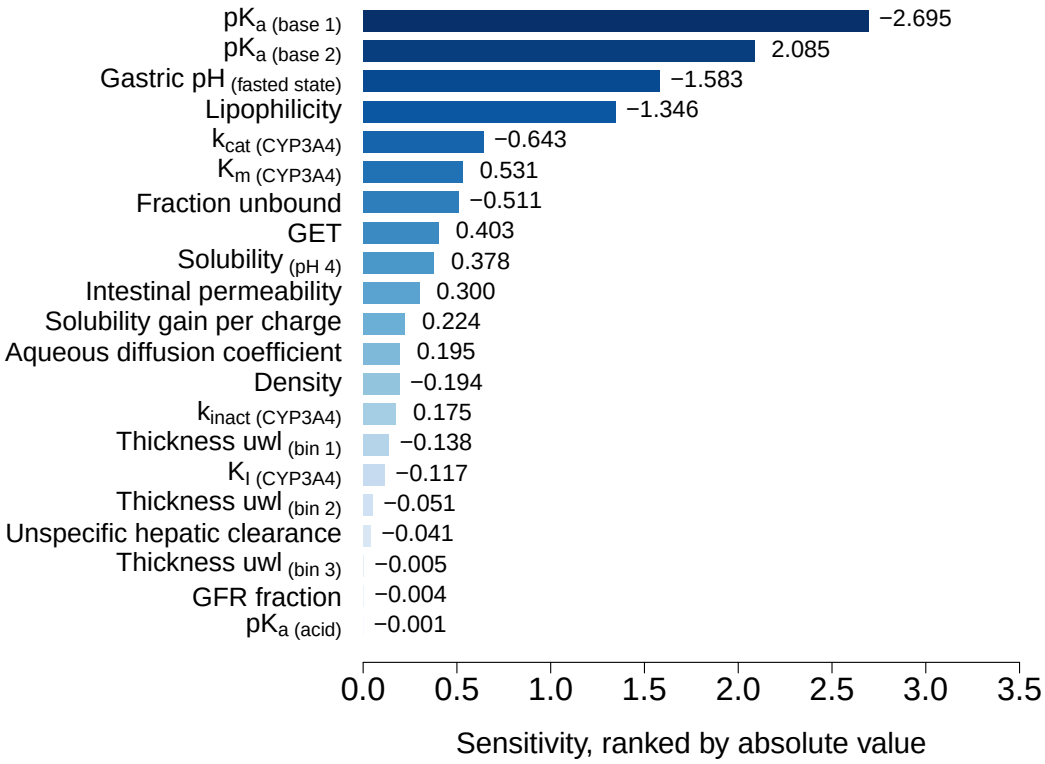

Figure S7: Sensitivity analysis of the dasatinib PBPK model. **CYP**: cytochrome P450, **GET**: gastric emptying time, **GFR**: glomerular filtration rate, $\mathbf{k_{cat}}$: catalytic rate constant, $\mathbf{K_I}$: inhibition constant, $\mathbf{k_{inact}}$: maximum rate of inactivation, $\mathbf{K_m}$: Michaelis-Menten constant, $\mathbf{pK_a}$: acid dissociation constant, **uwl**: unstirred water layer.

S3 PBPK Drug–Drug Interaction (DDI) Modeling

S3.1 Clinical DDI Studies

Table S7: Overview of clinical study data from the literature used for DDI model development.

Clinical study	Dosing of Perpetrator Drug	Dosing of Victim Drug	Gastric pH	N	Females [%]	Age [years]	BMI [kg/m^2]	Health Status	Dataset
(a) Enzyme-mediated DDIs									
	Ketoconazole	*Dasatinib*							
Johnson 2010 (control) [52]		20 mg, tab, qd, md (D1–D8)	2.0[a]	18	43	57.5 (23–80)[b]	-	cancer	test
Johnson 2010 (DDI) [52]	200 mg, tab, bid, md (D3–D8)	20 mg, tab, qd, md (D1–D8)	2.0[a]	18	43	57.5 (23–80)[b]	-	cancer	training
	Rifampicin	*Dasatinib*							
Study CA180032 (control) [6]		100 mg, tab, sd (D1)[c]	2.0[a]	20	-	-	-	healthy	test
Study CA180032 (DDI) [6]	600 mg, tab, qd, md (D2–D9)[d]	100 mg, tab, sd (D8)[c]	2.0[a]	20	-	-	-	healthy	test
	Dasatinib	*Simvastatin*							
Study CA180022 (control) [6]		80 mg, tab, sd (D1)	2.0[a]	48	58	40 (18–50)[e]	25.8 (20.9–31.7)[e]	healthy	test
Study CA180022 (DDI) [6]	100 mg, tab, sd (D8)	80 mg, tab, sd (D8)	2.0[a]	48	58	40 (18–50)[e]	25.8 (20.9–31.7)[e]	healthy	test
(b) pH-dependent DDIs									
	Rabeprazole	*Dasatinib*							
Yago 2014 (control) [51]		100 mg, tab, sd	0.6 (0.5–1.8)[b]	10	10	38 (23–59)[e]	- (21.6–29.1)	healthy	test
Yago 2014 (DDI (a)) [51]	20 mg, tab, bid, md (D1–D4)[f]	100 mg, tab, sd (D4)	4.1 (2.8–5.2)[e]	10	10	38 (23–59)[e]	- (21.6–29.1)	healthy	test
Yago 2014 (DDI (b)) [51]	20 mg, tab, bid, md (D1–D4)[f] + 1500 mg BHCl	100 mg, tab, sd (D4)[g]	0.7 (0.5–3.6)[e]	10	10	38 (23–59)[e]	- (21.6–29.1)	healthy	test

-: unknown, **bid**: twice a day, **BHCl**: betaine hydrochloride, **BMI**: body mass index, **D**: day, **DDI**: drug–drug interaction, **md**: multiple dose, **N**: number of participants, **qd**: once a day, **sd**: single dose, **tab**: tablet

[a] Default value in PK-Sim® for fasted state [11]

[b] Median (range)

[c] Administration of 100 mg dasatinib at 9:00 AM

[d] Administration of 600 mg rifampicin at 9:00 PM

[e] Mean (range)

[f] Single dose rabeprazole at D4

[g] Dasatinib administration following five minutes after BHCl administration

[h] Dasatinib was administered two hours before and ten hours after famotidine intake, respectively

[i] Dasatinib was administered two hours after and concomitantly with Maalox®, respectively

Table S7: Overview of clinical study data from the literature used for DDI model development *(continued)*.

Clinical study	Dosing of Perpetrator Drug	Dosing of Victim Drug	Gastric pH	N	Females [%]	Age [years]	BMI [kg/m^2]	Health Status	Dataset
	Famotidine	*Dasatinib*							
Eley 2009 (control) [50]		50 mg, tab, bid, md	2.0[a]	22	0	29 (19–47)[e]	25.1 (18.8–29.6)[e]	healthy	training
Eley 2009 (DDI (a)) [50]	40 mg, tab, bid, md	50 mg, tab, bid, md[h]	2.8 [53]	22	0	29 (19–47)[e]	25.1 (18.8–29.6)[e]	healthy	test
	Maalox®	*Dasatinib*							
Eley 2009 (control) [50]		50 mg, tab, bid, md	2.0[a]	22	0	29 (19–47)[e]	25.1 (18.8–29.6)[e]	healthy	training
Eley 2009 (DDI (b)) [50]	30 ml, liquid, bid, md	50 mg, tab, bid, md[i]	3.0 [54]	22	0	29 (19–47)[e]	25.1 (18.8–29.6)[e]	healthy	test

-: unknown, **bid**: twice a day, **BHCl**: betaine hydrochloride, **BMI**: body mass index, **D**: day, **DDI**: drug–drug interaction, **md**: multiple dose, **N**: number of participants, **qd**: once a day, **sd**: single dose, **tab**: tablet

[a] Default value in PK-Sim® for fasted state [11]

[b] Median (range)

[c] Administration of 100 mg dasatinib at 9:00 AM

[d] Administration of 600 mg rifampicin at 9:00 PM

[e] Mean (range)

[f] Single dose rabeprazole at D4

[g] Dasatinib administration following five minutes after BHCl administration

[h] Dasatinib was administered two hours before and ten hours after famotidine intake, respectively

[i] Dasatinib was administered two hours after and concomitantly with Maalox®, respectively

S3.2 DDI Model Evaluation

S3.2.1 Plasma Profiles of Enzyme-mediated DDIs (Semilogarithmic Scale)

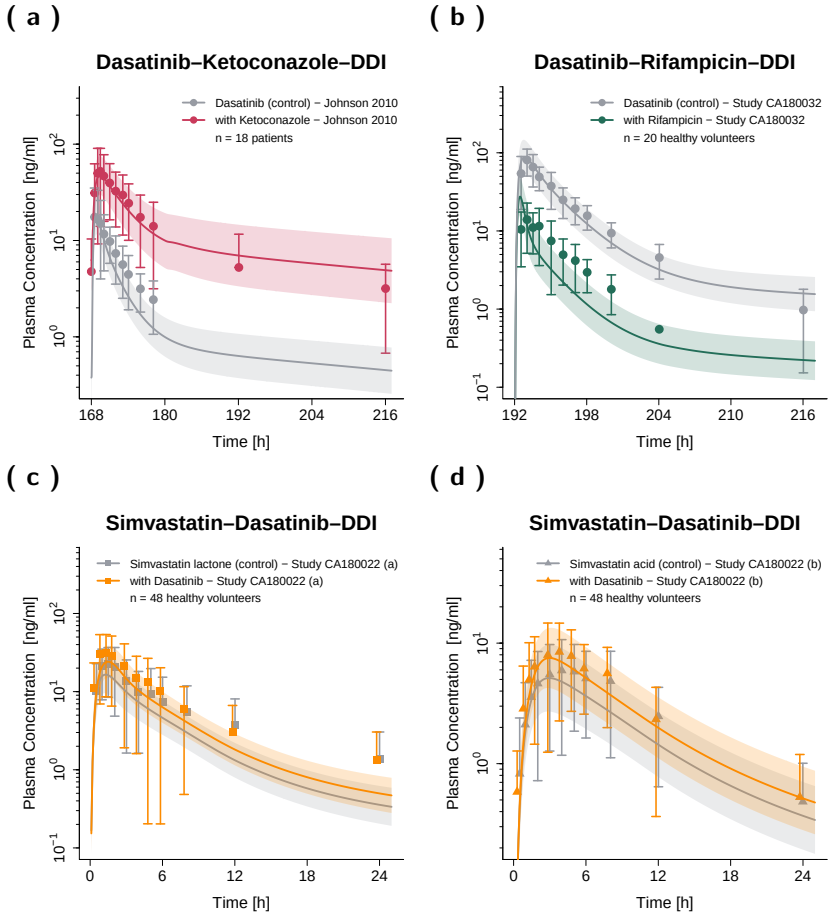

Figure S8: Predicted and observed plasma concentration–time profiles for enzyme-mediated DDIs with dasatinib acting as victim (a–b) and perpetrator drug (c–d) on a semilogarithmic scale. The solid lines show predicted geometric mean concentration–time profiles with and without intake of the perpetrator drug and ribbons show the corresponding geometric standard deviation of the population simulations (n=100). Points depict mean observed data and corresponding standard deviation of dasatinib, while squares and triangles depict the observed data and corresponding standard deviation of simvastatin lactone and simvastatin acid, respectively. /: no information available, **DDIs**: drug–drug interactions, **n**: number of participants.

S3.2.2 Plasma Profiles of pH-Dependent DDIs (Semilogarithmic Scale)

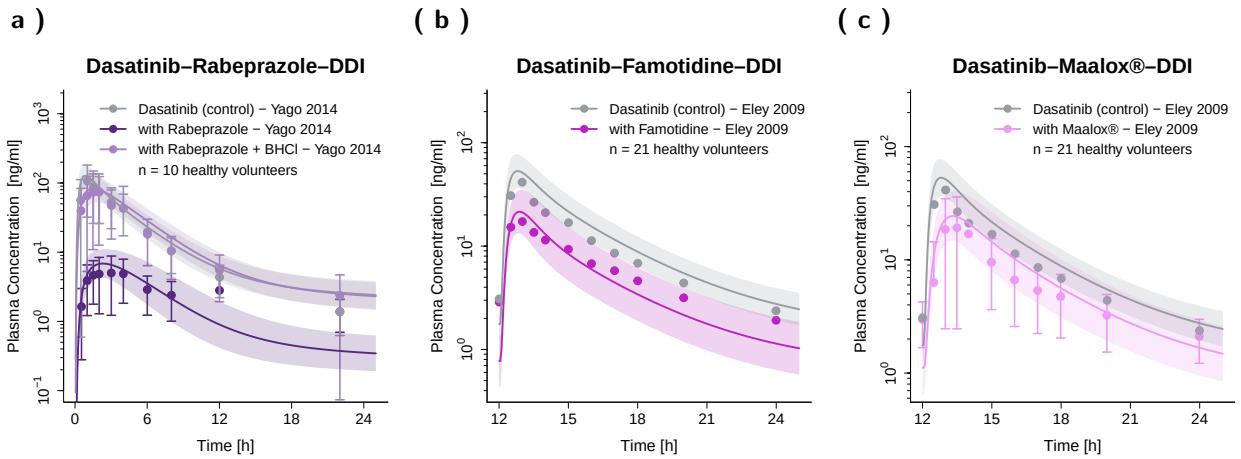

Figure S9: Predicted and observed plasma concentration–time profiles for the pH-dependent DDIs on a semilogarithmic scale. The solid lines show predicted geometric mean concentration–time profiles with and without the intake of perpetrator drug and ribbons show the corresponding geometric standard deviation of the population simulations (n=100). Points depict mean observed data and corresponding standard deviation of dasatinib (if depicted in the respective publication). **BHCl**: betaine hydrochloride, **DDIs**: drug–drug interactions, **n**: number of participants.

S3.2.3 Geometric Mean Fold Error (GMFE)

Table S8: Geometric Mean Fold Error (GMFE) of C_{max} and AUC_{last} DDI ratios.

		C_{max} DDI Ratio			**AUC_{last} DDI Ratio**			
Administration	Compound	Pred [1]	Obs [1]	Pred/Obs	Pred [1]	Obs [1]	Pred/Obs	Reference
Dasatinib–Ketoconazole–DDI	Dasatinib	2.17	2.99	0.73	9.14	7.65	1.19	Johnson 2010 [52]
Dasatinib–Rifampicin–DDI	Dasatinib	0.31	0.17	1.79	0.11	0.17	0.64	Study CA180032 [6]
Simvastatin–Dasatinib–DDI	Simvastatin lactone	1.48	1.38	1.07	1.47	1.23	1.20	Study CA180022 [6]
Simvastatin–Dasatinib–DDI	Simvastatin acid	1.52	1.43	1.06	1.45	1.19	1.22	Study CA180022 [6]
Dasatinib–Famotidine–DDI	Dasatinib	0.44	0.42	1.05	0.24	0.27	0.88	Eley 2009 [50]
Dasatinib–Maalox®–DDI	Dasatinib	0.45	0.46	0.97	0.31	0.28	1.09	Eley 2009 [50]
Dasatinib–Rabeprazole–DDI	Dasatinib	0.05	0.05	1.16	0.10	0.15	0.68	Yago 2014 [51]
Dasatinib–Rabeprazole–BHCl–DDI	Dasatinib	0.66	0.69	0.95	1.02	0.92	1.10	Yago 2014 [51]
		GMFE: 1.18 (1.03–1.79)			**GMFE: 1.24 (1.09–1.57)**			
		GMFE ≤ 2: 08/08			**GMFE ≤ 2: 08/08**			
		Guest limits: 08/08			**Guest limits: 08/08**			

AUC_{last}: area under the plasma concentration–time curve from the first to the last time point of measurement, **BHCl**: betaine hydrochloride, **C_{max}**: maximum plasma concentration, **DDI**: drug–drug interaction, **Obs**: observed, **Pred**: predicted

S4 PBPK Drug–Food Interaction (DFI) Modeling

S4.1 DFI Model Building

Studies have shown that the intake of both light and high-fat meals only marginally influences the pharmacokinetics (PK) of dasatinib. During light-fat meal ingestion, the maximum concentration (C_{max}) and area under the concentration–time curve (AUC) increased by 22% and 21%, respectively. The time to peak concentration (T_{max}) remained unaffected. In contrast, high-fat meal consumption led to a 24% decrease in C_{max} and a 14% increase in AUC, along with a one-hour delay in T_{max}, when compared to a fasted state [6]. The plasma concentration–time profiles of the DFI study investigating dasatinib exposure in the fasted state, after light-fat and high-fat breakfast were included in the model development (Table S9). The observed dasatinib data during ingestion of a light-fat meal (which only slightly impacted the PK of dasatinib) could be well predicted using the dasatinib model parameters of the fasted state, while the delay in T_{max} after a high-fat meal intake could be covered by prolonging the gastric emptying time from 15.0 minutes (default setting in PK-Sim® for the fasted state) to 103.4 minutes.

S4.1.1 Clinical DFI Studies

Table S9: Overview of clinical study data from the literature used for DFI model development.

Clinical study	Dosing of dasatinib	Meal	N	Females [%]	Age [years]	BMI [kg/m^2]	Health Status	Dataset
Study CA180009 (control)) [6]	100 mg, tab, qd, sd	Fasted state	48	-	-	-	healthy	test
Study CA180009 (DFI (a)) [6]	100 mg, tab, qd, sd	Light breakfast (319 kcal)	48	-	-	-	healthy	test
Study CA180009 (DFI (b)) [6]	100 mg, tab, qd, sd	High-fat breakfast (985 kcal)	48	-	-	-	healthy	test

BMI: body mass index, **D**: day, **DFI**: drug–food interaction, **N**: number of subjects, **qd**: once a day, **sd**: single dose, **tab**: tablet

S4.2 DFI Model Evaluation

S4.2.1 Plasma Profiles And Goodness-of-Fit Plot of DFIs

(a) **(b)**

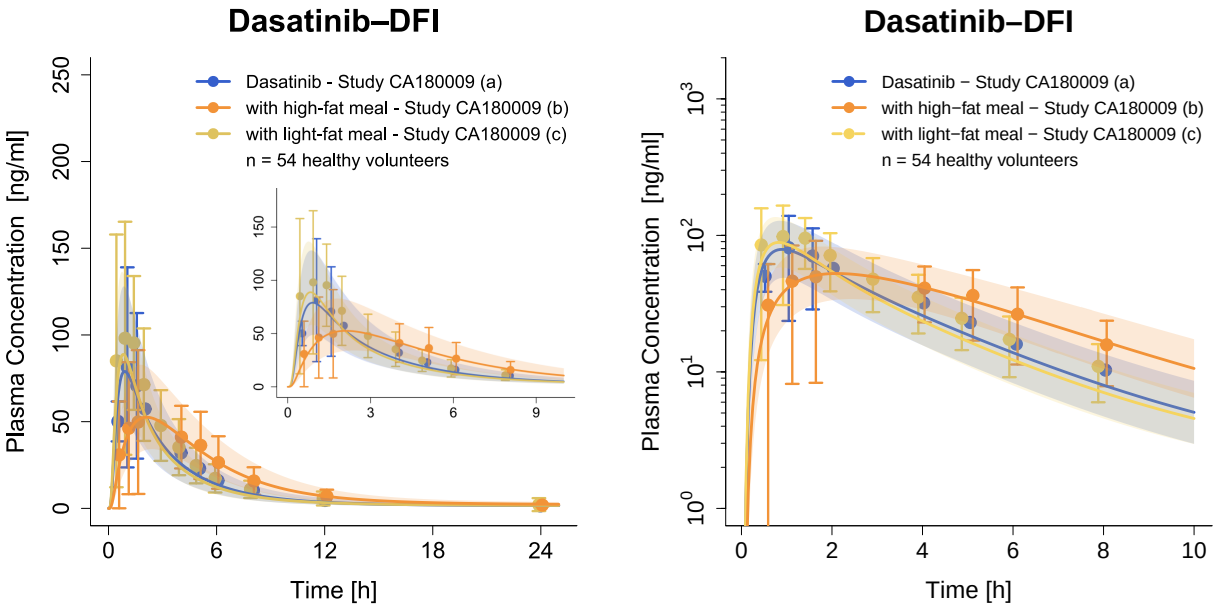

Figure S10: Predicted and observed plasma concentration–time profiles for the DFIs. Blue, yellow and orange lines show predicted geometric mean concentration–time profiles at fasted state, after light-fat and after high-fat breakfast, respectively. Ribbons show the corresponding geometric standard deviation of the population simulations (n=100). Points depict mean observed data and corresponding standard deviation of dasatinib. **DFI**: drug–food interaction, **n**: number of participants.

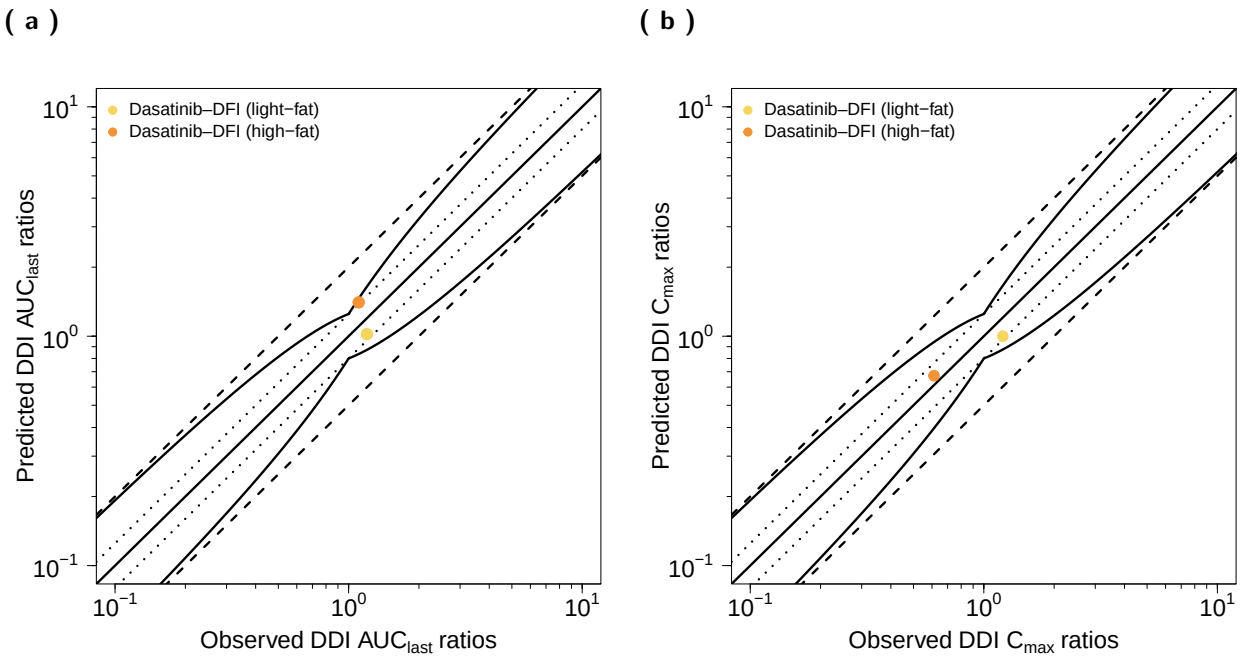

Figure S11: Predicted versus observed DFI AUC_{last} ratios (a) and DFI C_{max} ratios (b) of dasatinib. The straight solid lines mark the lines of identity, the curved lines show the limits of the predictive measure proposed by Guest et al. with 1.25-fold variability [55]. Dotted lines indicate 1.25-fold and dashed lines two-fold deviation. **AUC_{last}**: area under the plasma concentration–time curve from the first to the last time point of measurement, **C_{max}**: maximum plasma concentration, **DFI**: drug–food interaction.

S4.2.2 Geometric Mean Fold Error (GMFE)

Table S10: Geometric Mean Fold Error (GMFE) of C_{max} and AUC_{last} DFI ratios.

		C_{max} DFI Ratio			**AUC_{last} DFI Ratio**			
Administration	Compound	Pred [1]	Obs [1]	Pred/Obs	Pred [1]	Obs [1]	Pred/Obs	Reference
100 mg, po, tab, sd	Dasatinib	0.67	0.61	1.10	1.40	1.10	1.27	Study CA180009 (b) [6]
100 mg, po, tab, sd	Dasatinib	1.00	1.21	0.83	1.02	1.20	0.85	Study CA180009 (c) [6]
				GMFE: 1.15 (1.21–1.10)			**GMFE: 1.22 (1.17–1.27)**	
				GMFE ≤ 2: 02/02			**GMFE ≤ 2: 02/02**	
				Guest limits: 02/02			**Guest limits: 02/02**	

AUC_{last}: area under the plasma concentration–time curve from the first to the last time point of measurement, **C_{max}**: maximum plasma concentration, **DFI**, drug–food interaction, **Obs**: observed, **Pred**: predicted

S5 Model Application & Others

S5.1 Exposure Simulations for Model-Informed Precision Dosing

The developed PBPK model of dasatinib was coupled with previously published PBPK models of carbamazepine [56] (version 11), clarithomycin [24] (version 11), efavirenz [56, 57] (version 11), erythromycin [25] (version 11), fluconazole [20] (version 11), fluvoxamine [58] (version 11), grapefruit juice [59] (version 11), itraconazole [24] (version 11), ketoconazole [60] (version 11), rifampicin [24] (version 11), simvastatin [21] (version 9) and voriconazole [61] (version 11). The drug-dependent parameters of the compounds were adapted from the respective publications. Modifications of drug-dependent parameters are shown in Table S11.

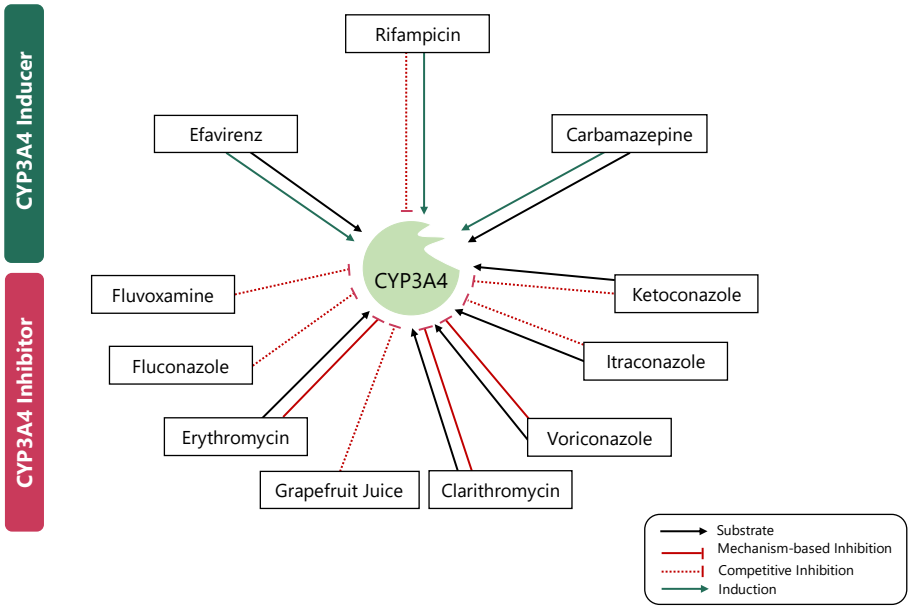

Figure S12: Overview of investigated DDI scenarios. The developed dasatinib PBPK model was coupled with previously published PBPK perpetrator models of clarithromycin, erythromycin, fluconazole, fluvoxamine, grapefruit juice, itraconazole, ketoconazole and voriconazole as CYP3A4 inhibitors as well as of carbamazepine, efavirenz and rifampicin as CYP3A4 inducers. **DDI:** drug–drug interaction, **PBPK:** physiologically based pharmacokinetic.

Table S11: Modified drug-dependent parameters of the PBPK models from the literature.

PBPK model	Modified parameter	Published parameter	Reason for Modification
Efavirenz [56, 57]	modified according to [56]	see [57]	-
Erythromycin [25]	OATP1B1 k_{cat} = 19.29 1/min	OATP1B1 k_{cat} = 1.35 1/min	Different OATP1B1 ref. conc.
Rifampicin [24]	OATP1B1 k_{cat} = 74.43 1/min	OATP1B1 k_{cat} = 5.21 1/min	Different OATP1B1 ref. conc.
Simvastatin [21]	OATP1B1 k_{cat} = 146.41 1/min	OATP1B1 k_{cat} = 10.25 1/min	Different OATP1B1 ref. conc.

k_{cat}: catalytic rate constant, **OATP**: organic anion transporting polypeptide, **ref. conc.**: reference concentration

Table S12: Overview of model-based dose adaptations for dasatinib within various DDI scenarios based on the exposure matching principle.

Perpetrator	Dosing of Perpetrator	Dosing of Dasatinib	AUC_{ss} Ratio[1]	AUC_{ss} Ratio[2] (adapted)	Adapted Dasatinib Dose
Strong CYP3A4 Inhibitors					
Clarithromycin	250 mg, bid	100 mg, qd	1.85	0.99	50 mg, qd
	250 mg, bid	140 mg, qd	1.76	0.96	70 mg, qd
Clarithromycin	500 mg, bid	100 mg, qd	3.37	1.11	30 mg, qd
	500 mg, bid	140 mg, qd	3.21	1.05	40 mg, qd
Itraconazole	200 mg, bid	100 mg, qd	4.59	1.03	20 mg, qd
(fed state)	200 mg, bid	140 mg, qd	4.36	1.09	30 mg, qd
Ketoconazole	200 mg, bid	100 mg, qd	3.75	0.84	20 mg, qd
	200 mg, bid	140 mg, qd	3.59	0.88	30 mg, qd
Voriconazole	400 mg, qd (D1) + 200 mg, bid	100 mg, qd	3.01	0.98	30 mg, qd
	400 mg, qd (D1) + 200 mg, bid	140 mg, qd	2.87	0.93	40 mg, qd
Moderate CYP3A4 Inhibitors					
Erythromycin	500 mg, tid	100 mg, qd	2.12	0.93	40 mg, qd
	500 mg, tid	140 mg, qd	1.84	0.97	60 mg, qd
Erythromycin	500 mg, qid	100 mg, qd	2.31	1.01	40 mg, qd
	500 mg, qid	140 mg, qd	2.19	1.05	60 mg, qd
Fluconazole	200 mg, qd	100 mg, qd	2.11	1.09	50 mg, qd
	200 mg, qd	140 mg, qd	2.04	0.93	60 mg, qd
Fluconazole	400 mg, qd	100 mg, qd	2.70	0.87	30 mg, qd
	400 mg, qd	140 mg, qd	2.59	1.01	50 mg, qd
Fluvoxamine	100 mg, qd	100 mg, qd	1.15	1.04	90 mg, qd
(+0 h)	100 mg, qd	140 mg, qd	1.12	0.98	120 mg, qd

-: Dose adaptations could not be provided, **AUC_{ss}**:, steady state area under the concentration–time curve, **bid**: twice a day, **D**: day, **IR**: immediate release, **qd**: once daily, **qid**: four times a day, **sd**: single dose, **tab**: tablet, **tid**: three times a day

[1] AUC_{ss} Ratio was calculated dividing AUC_{ss} of the DDI setting (with 100 or 140 mg dasatinib) by the corresponding AUC_{ss} of the control scenario.

[2] AUC_{ss} Ratio (adapted) was calculated dividing AUC_{ss} of the DDI setting using the model-based adapted dose of dasatinib by the corresponding AUC_{ss} of the control scenario.

[3] Rifampicin is also a weak CYP3A4 inhibitor; administrations were simulated to be concomitantly with dasatinib administrations.

Table S12: Overview of model-based dose adaptations for dasatinib within various DDI scenarios based on the exposure matching principle.

Perpetrator	**Dosing of Perpetrator**	**Dosing of Dasatinib**	**AUC_{ss} Ratio**	**AUC_{ss} Ratio (adapted)**	**Adapted Dasatinib Dose**
Fluvoxamine	100 mg, qd	100 mg, qd	1.02	1.02	100 mg, qd
(+12 h)	100 mg, qd	140 mg, qd	1.02	1.02	140 mg, qd
Grapefruit Juice	250 ml, qd	100 mg, qd	1.40	1.02	70 mg, qd
	250 ml, qd	140 mg, qd	1.33	1.00	100 mg, qd
Grapefruit Juice	250 ml, sd	100 mg, qd	1.13	1.02	90 mg, qd
	250 ml, sd	140 mg, qd	1.10	1.03	130 mg, qd
Strong CYP3A4 Inducers					
Carbamazepine	400 mg, tid	100 mg, qd	0.30	1.01	250 mg, qd
(IR tab, fed state)	400 mg, tid	140 mg, qd	0.35	0.99	340 mg, qd
Rifampicin[3]	600 mg, qd	100 mg, qd	0.50	1.01	230 mg, qd
	600 mg, qd	140 mg, qd	0.48	1.00	360 mg, qd
Moderate CYP3A4 Inducers					
Efavirenz	600 mg, qd	100 mg, qd	0.34	0.99	240 mg, qd
(+ 0 h)	600 mg, qd	140 mg, qd	0.37	1.00	340 mg, qd
Efavirenz	600 mg, qd	100 mg, qd	0.23	1.00	310 mg, qd
(+12 h)	600 mg, qd	140 mg, qd	-	-	-

-: Dose adaptations could not be provided, **AUC_{ss}**:, steady state area under the concentration–time curve, **bid**: twice a day, **D**: day, **IR**: immediate release, **qd**: once daily, **qid**: four times a day, **sd**: single dose, **tab**: tablet, **tid**: three times a day

[1] AUC_{ss} Ratio was calculated dividing AUC_{ss} of the DDI setting (with 100 or 140 mg dasatinib) by the corresponding AUC_{ss} of the control scenario.

[2] AUC_{ss} Ratio (adapted) was calculated dividing AUC_{ss} of the DDI setting using the model-based adapted dose of dasatinib by the corresponding AUC_{ss} of the control scenario.

[3] Rifampicin is also a weak CYP3A4 inhibitor; administrations were simulated to be concomitantly with dasatinib administrations.

S5.1.1 Plasma Profiles of Simulated Single DDI Scenarios

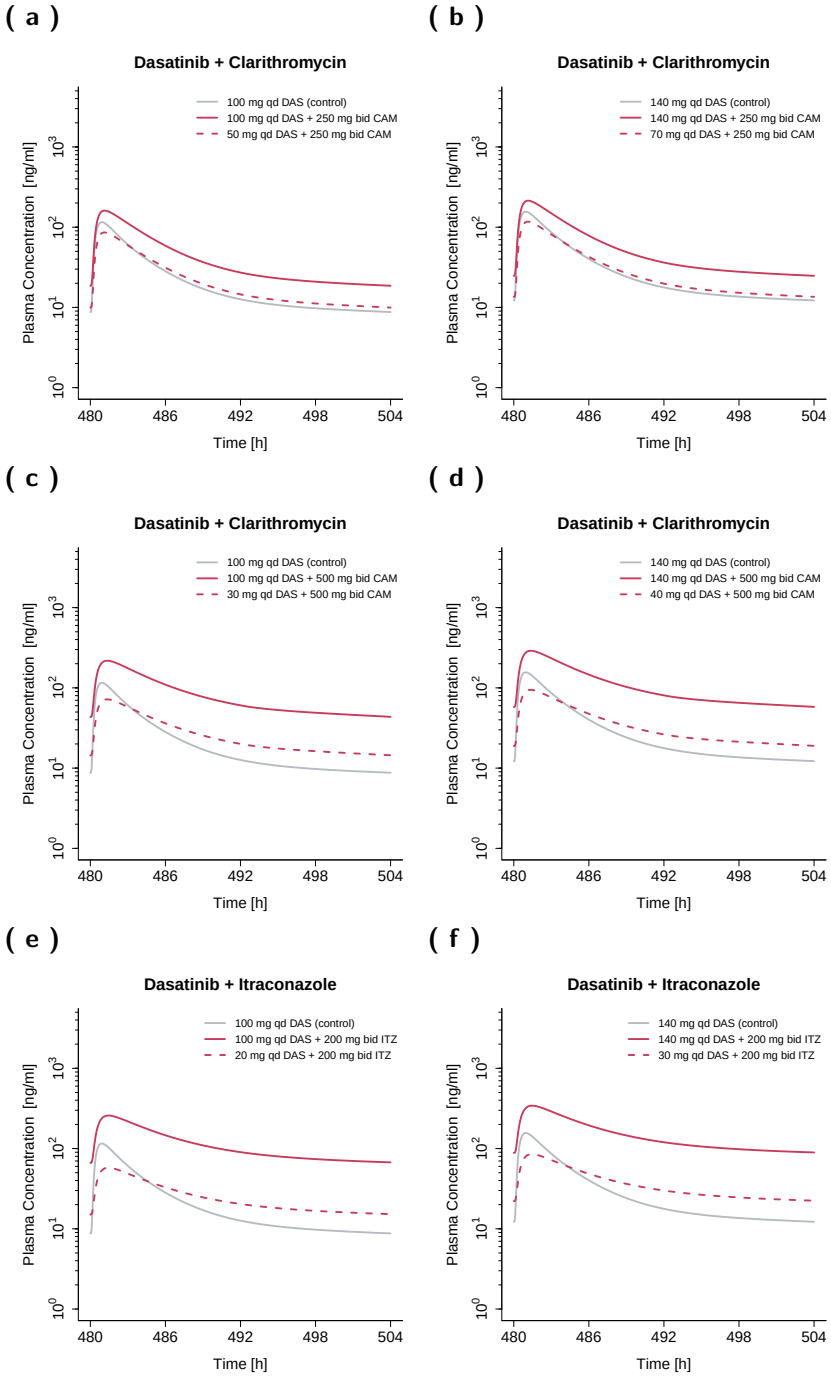

Figure S13: Model-based dose adaptations for dasatinib within various single DDI scenarios including moderate and strong CYP3A4 inhibitors and inducers. The first and second column represent the simulation results after administration of 100 mg and 140 mg dasatinib daily, respectively. Colored and grey solid lines show simulated mean concentration–time profiles with and without intake of a perpetrator drug, respectively. Dashed lines represent the simulated mean concentration–time profiles in presence of a perpetrator drug, using an adapted dose of dasatinib. **Bid**: twice a day, **CAM**: clarithromycin, **CBZ**: carbamazepine, **D**: day, **DAS**: dasatinib, **DDI**: drug–drug interaction, **EFV**: efavirenz, **ERY**: erythromycin, **FLV**: fluvoxamine, **FLZ**: fluconazole, **GFJ**: grapefruit juice, **ITZ**: itraconazole, **KCZ**: ketoconazole, **qd**: once a day, **qid**: four times a day, **RIF**: rifampicin, **sd**: single dose, **tid**: three times a day, **VRC**: voriconazole.

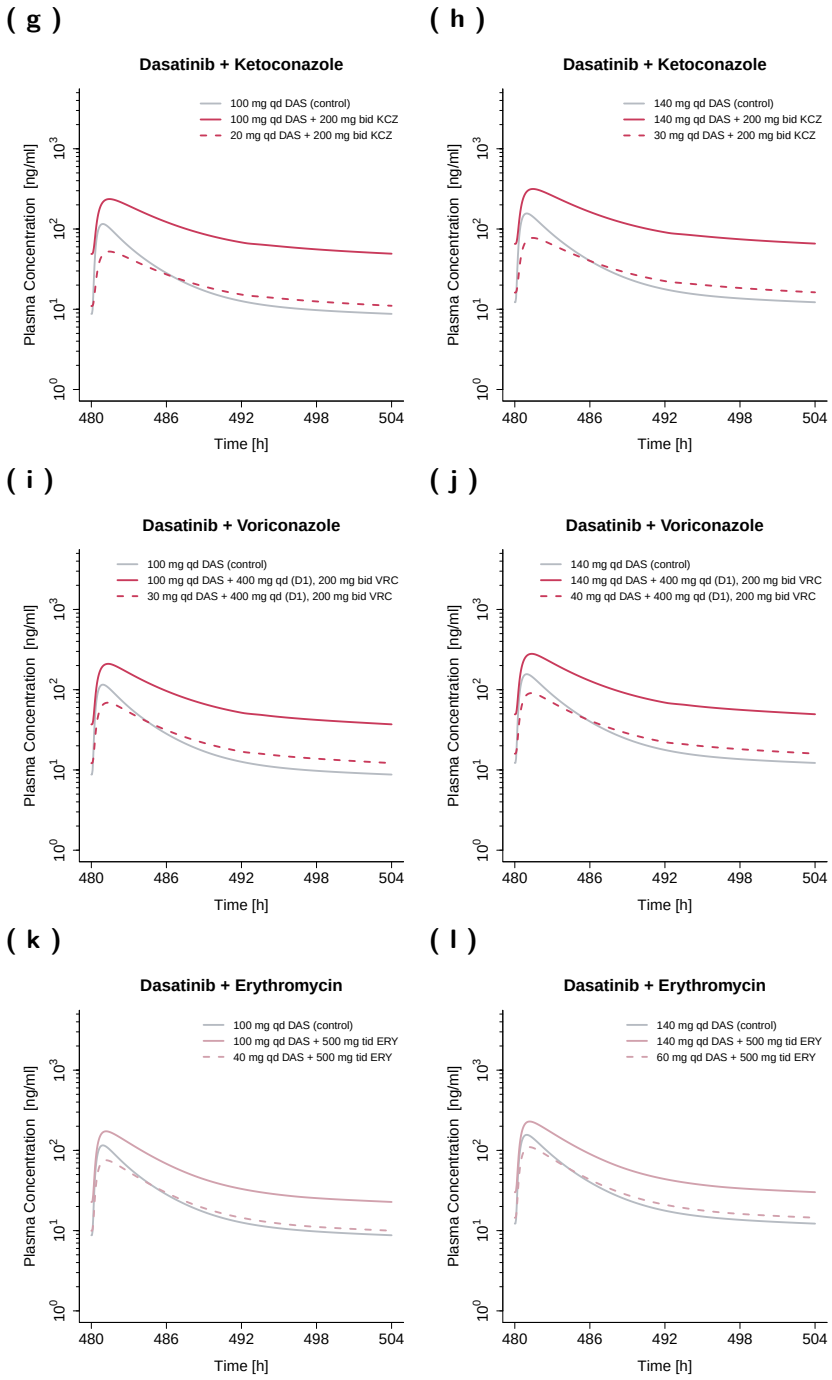

Figure S13: *(continued)* **Model-based dose adaptations for dasatinib within various single DDI scenarios including moderate and strong CYP3A4 inhibitors and inducers.** The first and second column represent the simulation results after administration of 100 mg and 140 mg dasatinib daily, respectively. Colored and grey solid lines show simulated mean concentration–time profiles with and without intake of a perpetrator drug, respectively. Dashed lines represent the simulated mean concentration–time profiles in presence of a perpetrator drug, using an adapted dose of dasatinib. **Bid**: twice a day, **CAM**: clarithromycin, **CBZ**: carbamazepine, **D**: day, **DAS**: dasatinib, **DDI**: drug–drug interaction, **EFV**: efavirenz, **ERY**: erythromycin, **FLV**: fluvoxamine, **FLZ**: fluconazole, **GFJ**: grapefruit juice, **ITZ**: itraconazole, **KCZ**: ketoconazole, **qd**: once a day, **qid**: four times a day, **RIF**: rifampicin, **sd**: single dose, **tid**: three times a day, **VRC**: voriconazole.

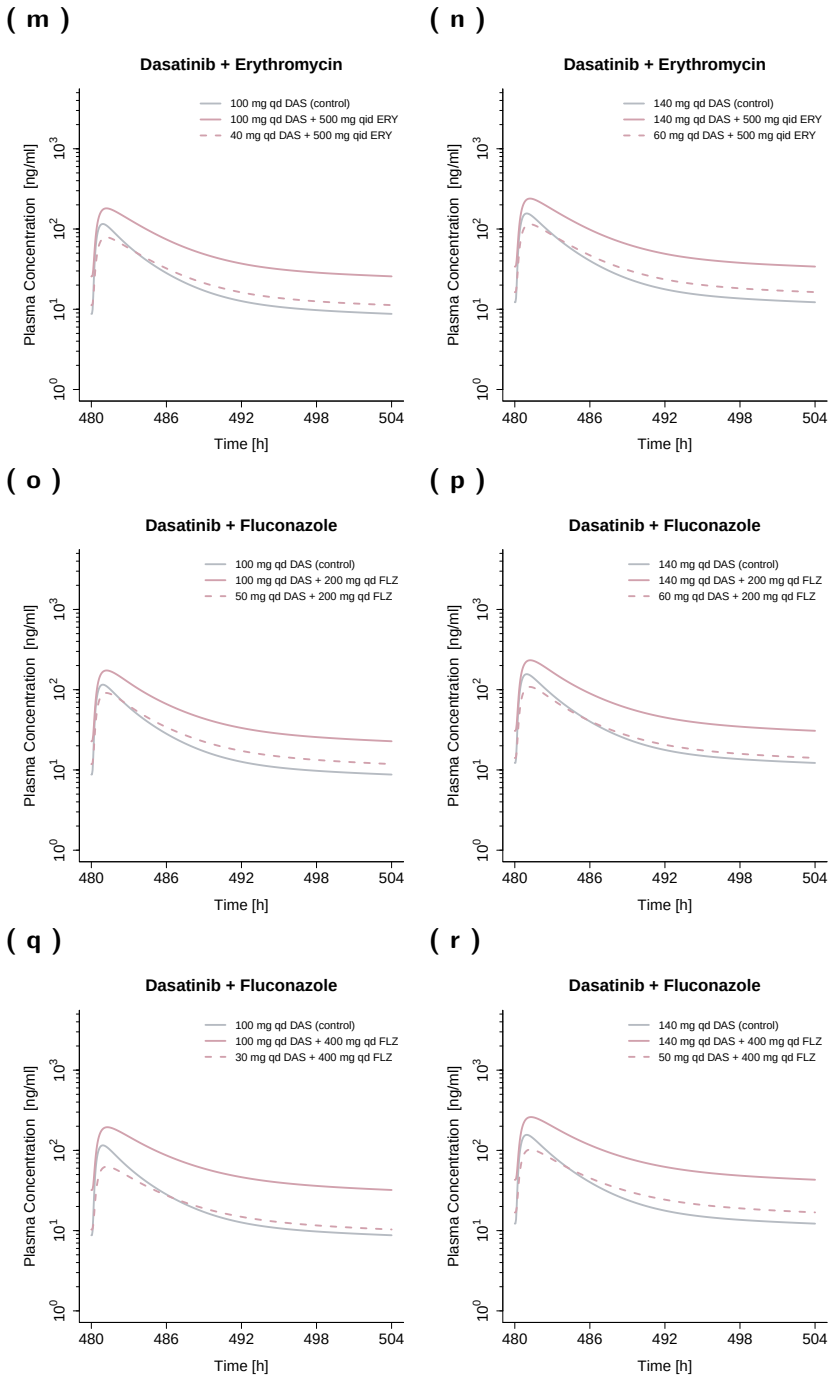

Figure S13: *(continued)* **Model-based dose adaptations for dasatinib within various single DDI scenarios including moderate and strong CYP3A4 inhibitors and inducers.** The first and second column represent the simulation results after administration of 100 mg and 140 mg dasatinib daily, respectively. Colored and grey solid lines show simulated mean concentration–time profiles with and without intake of a perpetrator drug, respectively. Dashed lines represent the simulated mean concentration–time profiles in presence of a perpetrator drug, using an adapted dose of dasatinib. **Bid**: twice a day, **CAM**: clarithromycin, **CBZ**: carbamazepine, **D**: day, **DAS**: dasatinib, **DDI**: drug–drug interaction, **EFV**: efavirenz, **ERY**: erythromycin, **FLV**: fluvoxamine, **FLZ**: fluconazole, **GFJ**: grapefruit juice, **ITZ**: itraconazole, **KCZ**: ketoconazole, **qd**: once a day, **qid**: four times a day, **RIF**: rifampicin, **sd**: single dose, **tid**: three times a day, **VRC**: voriconazole.

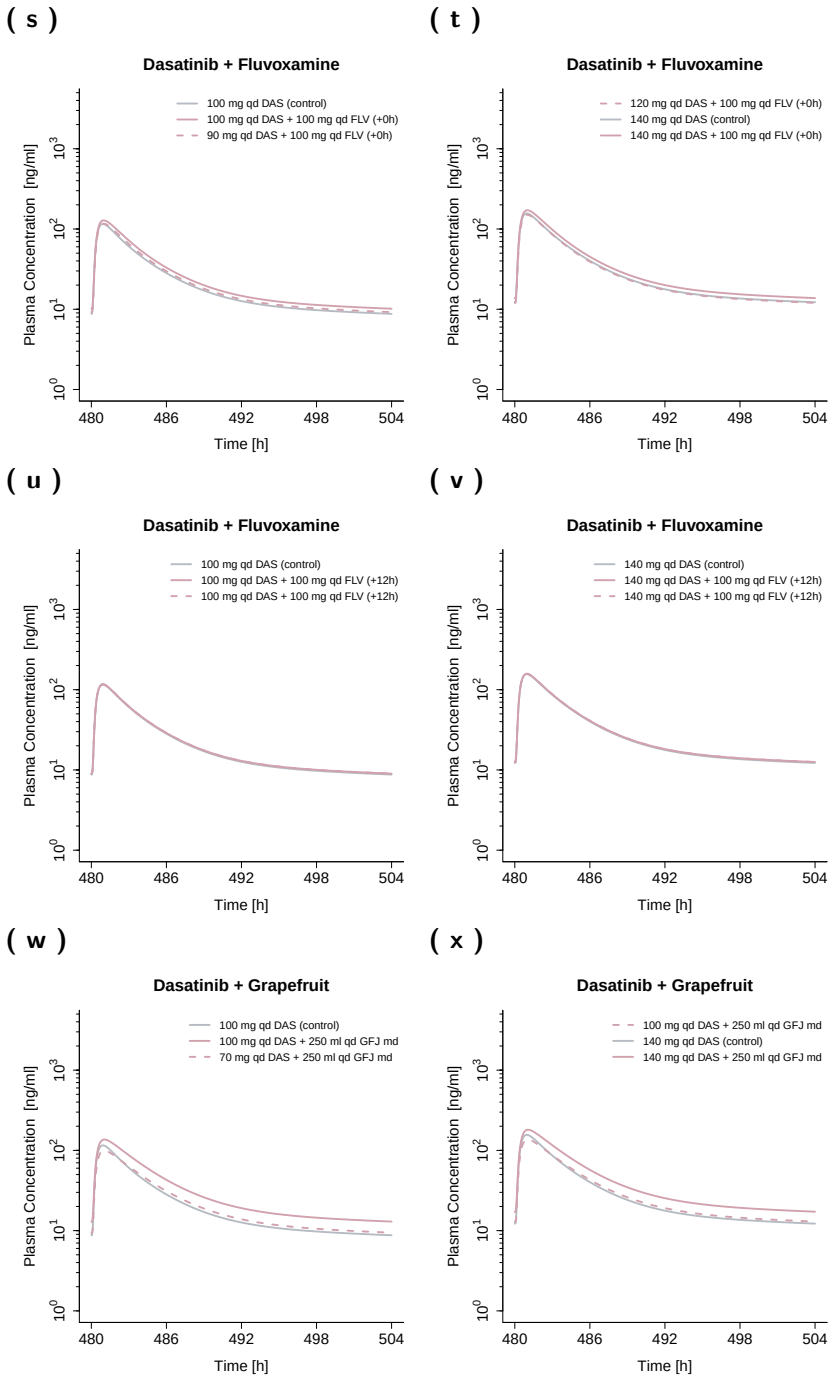

Figure S13: *(continued)* **Model-based dose adaptations for dasatinib within various single DDI scenarios including moderate and strong CYP3A4 inhibitors and inducers.** The first and second column represent the simulation results after administration of 100 mg and 140 mg dasatinib daily, respectively. Colored and grey solid lines show simulated mean concentration–time profiles with and without intake of a perpetrator drug, respectively. Dashed lines represent the simulated mean concentration–time profiles in presence of a perpetrator drug, using an adapted dose of dasatinib. **Bid**: twice a day, **CAM**: clarithromycin, **CBZ**: carbamazepine, **D**: day, **DAS**: dasatinib, **DDI**: drug–drug interaction, **EFV**: efavirenz, **ERY**: erythromycin, **FLV**: fluvoxamine, **FLZ**: fluconazole, **GFJ**: grapefruit juice, **ITZ**: itraconazole, **KCZ**: ketoconazole, **qd**: once a day, **qid**: four times a day, **RIF**: rifampicin, **sd**: single dose, **tid**: three times a day, **VRC**: voriconazole.

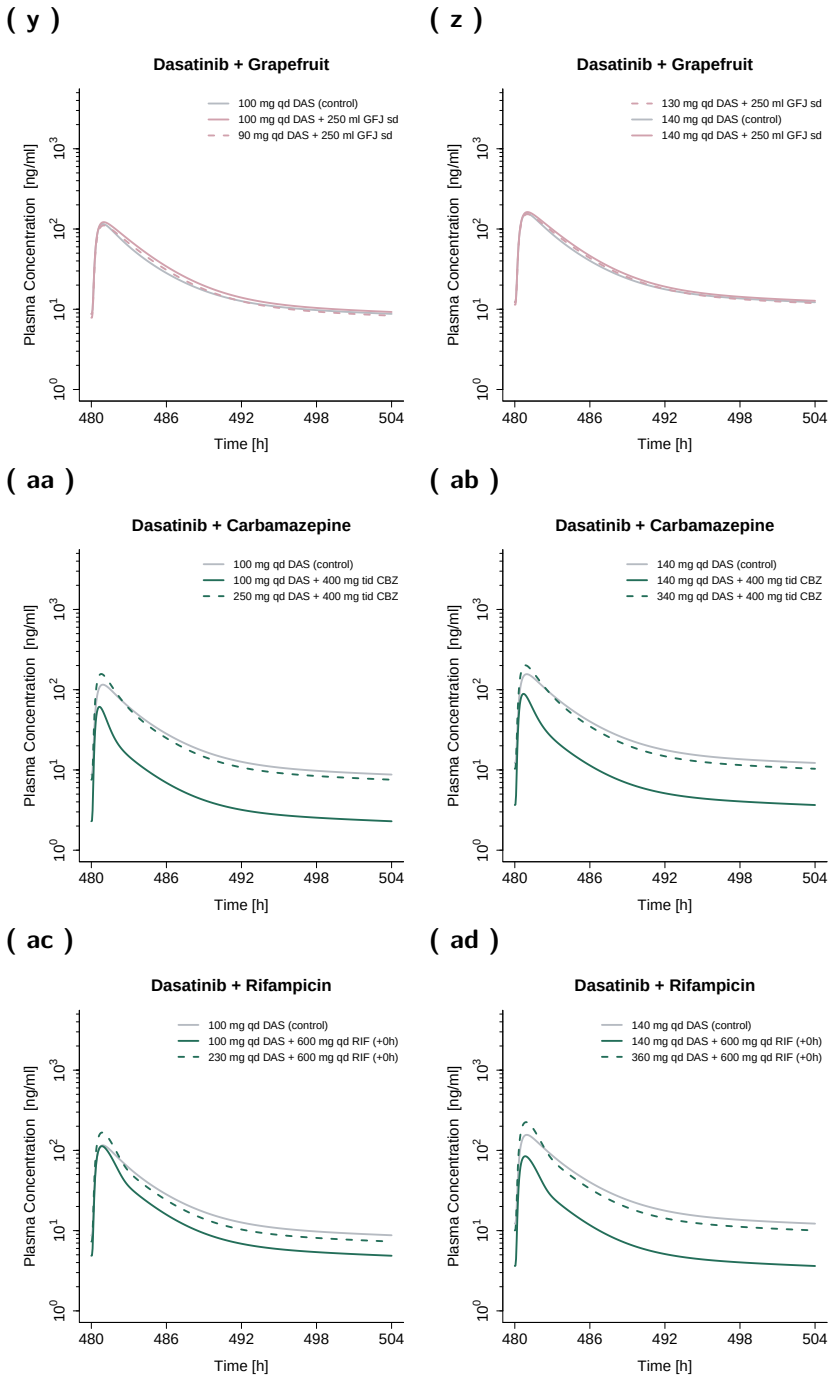

Figure S13: *(continued)* **Model-based dose adaptations for dasatinib within various single DDI scenarios including moderate and strong CYP3A4 inhibitors and inducers.** The first and second column represent the simulation results after administration of 100 mg and 140 mg dasatinib daily, respectively. Colored and grey solid lines show simulated mean concentration–time profiles with and without intake of a perpetrator drug, respectively. Dashed lines represent the simulated mean concentration–time profiles in presence of a perpetrator drug, using an adapted dose of dasatinib. **Bid**: twice a day, **CAM**: clarithromycin, **CBZ**: carbamazepine, **D**: day, **DAS**: dasatinib, **DDI**: drug–drug interaction, **EFV**: efavirenz, **ERY**: erythromycin, **FLV**: fluvoxamine, **FLZ**: fluconazole, **GFJ**: grapefruit juice, **ITZ**: itraconazole, **KCZ**: ketoconazole, **qd**: once a day, **qid**: four times a day, **RIF**: rifampicin, **sd**: single dose, **tid**: three times a day, **VRC**: voriconazole.

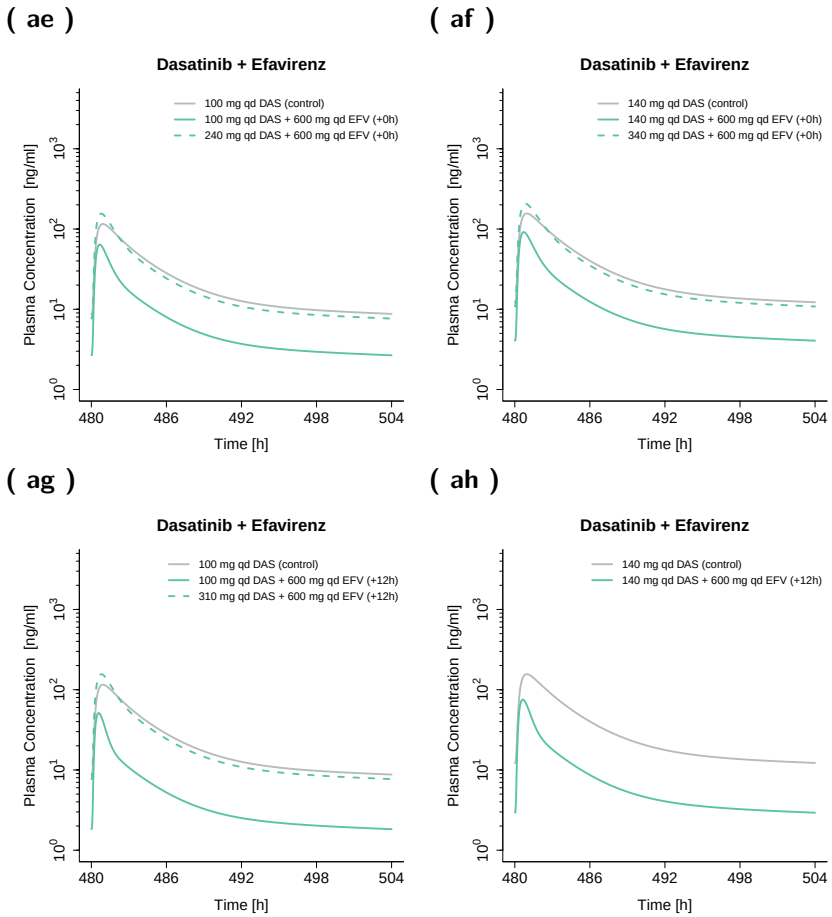

Figure S13: *(continued)* **Model-based dose adaptations for dasatinib within various single DDI scenarios including moderate and strong CYP3A4 inhibitors and inducers.** The first and second column represent the simulation results after administration of 100 mg and 140 mg dasatinib daily, respectively. Colored and grey solid lines show simulated mean concentration–time profiles with and without intake of a perpetrator drug, respectively. Dashed lines represent the simulated mean concentration–time profiles in presence of a perpetrator drug, using an adapted dose of dasatinib. **Bid**: twice a day, **CAM**: clarithromycin, **CBZ**: carbamazepine, **D**: day, **DAS**: dasatinib, **DDI**: drug–drug interaction, **EFV**: efavirenz, **ERY**: erythromycin, **FLV**: fluvoxamine, **FLZ**: fluconazole, **GFJ**: grapefruit juice, **ITZ**: itraconazole, **KCZ**: ketoconazole, **qd**: once a day, **qid**: four times a day, **RIF**: rifampicin, **sd**: single dose, **tid**: three times a day, **VRC**: voriconazole.

S5.1.2 Plasma Profiles of Simulated Multiple DDI Scenarios

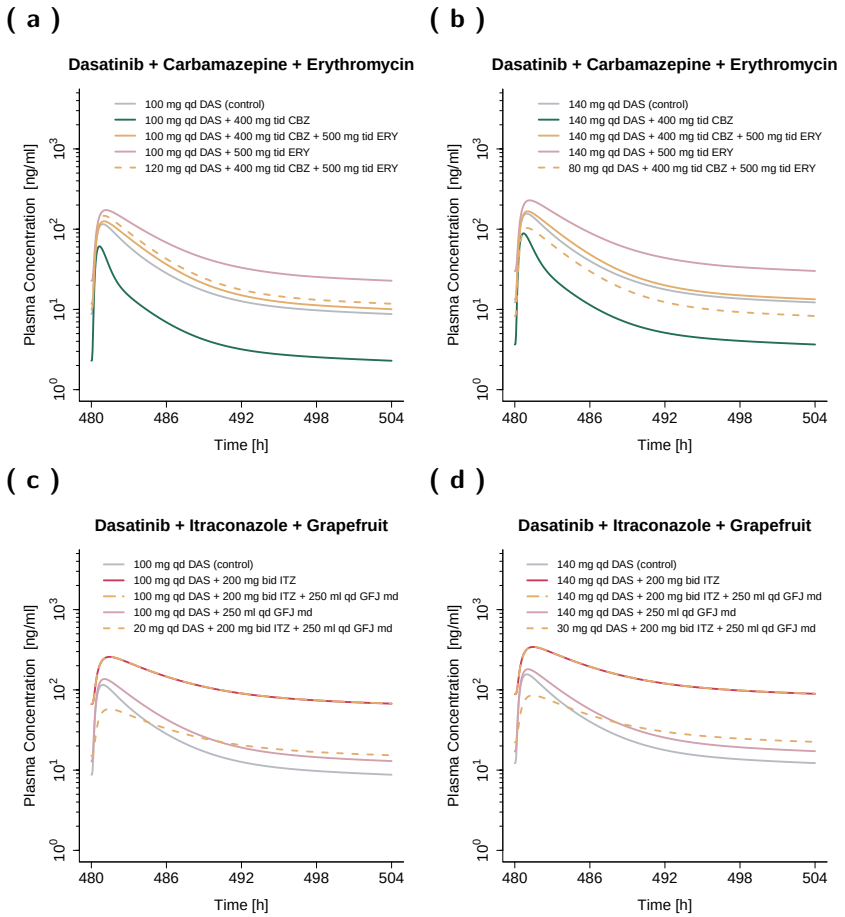

Figure S14: Model-based dose adaptations for dasatinib within multiple DDIs. The first and second column represent the simulation results after administration of 100 mg and 140 mg dasatinib daily, respectively. Colored and grey solid lines show simulated mean concentration–time profiles with and without intake of perpetrator drug(s), respectively. Dashed lines represent the simulated mean concentration–time profiles in presence of perpetrator drug(s), using an adapted dose of dasatinib. **Bid**: twice a day, **CBZ**: carbamazepine, **DAS**: dasatinib, **DDI**: drug–drug interaction, **ERY**: erythromycin, **GFJ**: grapefruit juice, **ITZ**: itraconazole, **qd**: once a day, **tid**: three times a day.

S5.2 CYP3A4 Autoinhibition

Dasatinib exhibits time-dependent inhibition of CYP3A4 according to *in vitro* studies [44, 62] affecting the exposure of CYP3A4 substrates (e.g., simvastatin) [6], but also its own metabolism. CYP3A4 time-dependent inhibition by dasatinib results in a slight supra-proportional increase in exposure of 16% comparing area under the concentration–time curve (AUC) from zero to infinity after single dose administration and AUC steady state (AUC_{ss}) (see Table S13). Moreover, the time-dependent inhibition showed no or only minor effects on the performed prospective DDI simulations with dasatinib as victim drug (e.g., no impact on AUC_{ss} during itraconazole DDI and 7% higher AUC_{ss} during fluvoxamine DDI).

Table S13: Impact of CYP3A4 autoinhibition on dasatinib exposure.

Dasatinib Dosing Regimen	AUC_{inf}	AUC_{ss}	AUC_{ss}/AUC_{inf}
20 mg, sd	0.19	-	1.07
20 mg, qd	-	0.20	1.07
100 mg, sd	1.06	-	1.16
100 mg, qd	-	1.24	1.16
140 mg, sd	1.51	-	1.15
140 mg, qd	-	1.73	1.15
360 mg, sd	3.09	-	1.11
360 mg, qd	-	3.42	1.11
420 mg, sd	3.26	-	1.10
420 mg, qd	-	3.58	1.10

AUC_{inf}: area under the concentration–time curve from zero to infinity,
AUC_{ss}:, steady state area under the concentration–time curve,
CYP: cytochrome P450, **qd**: once a day, **sd**: single dose

S5.3 Pharmacokinetic Parameters: Absolute Bioavailability, Fraction Absorbed, Fraction Metabolized, Fraction Escaping Gut Wall and Hepatic Elimination

Table S14: Overview of simulated F_a, F_g, F_h, F_m and BA.

Dasatinib Dosing Regimen	F_a (%)	F_g (%)	F_h (%)	F_m (%)	BA (%)
20 mg, sd	80	47	64	94	24
100 mg, sd	69	64	63	93	28
140 mg, sd	65	68	63	92	28
360 mg, sd	45	79	62	91	22
420 mg, sd	41	79	62	90	20

BA: absolute bioavailability, **CYP**: cytochrome P450, **F_a**: fraction absorbed,
F_g: fraction escaping gut wall elimination, **F_h**: fraction escaping hepatic elimination
F_m: fraction metabolized via CYP3A4, **sd**: single dose

References

[1] National Center for Health Statistics (1997) Third National Health and Nutrition Examination Survey (NHANES III). Tech. rep., Hyattsville, MD 20782

[2] Amercian Cancer Society (2022) Cancer Facts and Figures. https://www.cancer.org/cancer/chronic-myeloid-leukemia/about/statistics.html, available online (accessed: 2023-02-01)

[3] Valentin J (2002) Basic anatomical and physiological data for use in radiological protection: reference values. A report of age- and gender-related differences in the anatomical and physiological characteristics of reference individuals. ICRP Publication 89. Annals of the ICRP 32(3-4):5–265

[4] Schlender J (2015) A report including the description of the physiology base of the Japenese population implemented in PK-Sim®. https://github.com/Open-Systems-Pharmacology/OSPSuite.Documentation/blob/master/Japanese_Population/Report.md, available online (accessed: 2022-08-04)

[5] Willmann S, Höhn K, Edginton A, Sevestre M, Solodenko J, Weiss W, Lippert J, Schmitt W (2007) Development of a physiology-based whole-body population model for assessing the influence of individual variability on the pharmacokinetics of drugs. Journal of pharmacokinetics and pharmacodynamics 34(3):401–31

[6] Center for Drug Evaluation (2005) Clinical Pharmacology and Biopharmaceutics Review(s): NDA Review - Dasatinib. https://www.accessdata.fda.gov/drugsatfda_docs/nda/2006/021986s000_Sprycel__ClinPharmR.pdf, available online (accessed: 2022-08-04)

[7] Christopher LJ, Cui D, Wu C, Luo R, Manning JA, Bonacorsi SJ, Lago M, Allentoff A, Lee FYF, McCann B, Galbraith S, Reitberg DP, He K, Barros A, Blackwood-Chirchir A, Humphreys WG, Iyer RA (2008) Metabolism and disposition of dasatinib after oral administration to humans. Drug metabolism and disposition: the biological fate of chemicals 36(7):1357–64

[8] Vaidhyanathan S, Wang X, Crison J, Varia S, Gao JZH, Saxena A, Good D (2019) Bioequivalence Comparison of Pediatric Dasatinib Formulations and Elucidation of Absorption Mechanisms Through Integrated PBPK Modeling. Journal of pharmaceutical sciences 108(1):741–749

[9] Vargas M, Villarraga E (2016) Bioequivalence Study of Two Dasatinib 100 mg Formulations in Healthy Colombians. Journal of Bioequivalence & Bioavailability 09(01):302–305

[10] Luo FR, Barrett YC, Yang Z, Camuso A, McGlinchey K, Wen ML, Smykla R, Fager K, Wild R, Palme H, Galbraith S, Blackwood-Chirchir A, Lee FY (2008) Identification and validation of phospho-SRC, a novel and potential pharmacodynamic biomarker for dasatinib (SPRYCEL), a multi-targeted kinase inhibitor. Cancer chemotherapy and pharmacology 62(6):1065–74

[11] Willmann S, Schmitt W, Keldenich J, Lippert J, Dressman JB (2004) A physiological model for the estimation of the fraction dose absorbed in humans. Journal of medicinal chemistry 47(16):4022–31

[12] Zwaan CM, Rizzari C, Mechinaud F, Lancaster DL, Lehrnbecher T, van der Velden VHJ, Beverloo BB, den Boer ML, Pieters R, Reinhardt D, Dworzak M, Rosenberg J, Manos G, Agrawal S, Strauss L, Baruchel A, Kearns PR (2013) Dasatinib in children and adolescents with relapsed or refractory leukemia: results of the CA180-018 phase I dose-escalation study of the Innovative Therapies for Children with Cancer Consortium. Journal of clinical oncology : official journal of the American Society of Clinical Oncology 31(19):2460–8

[13] Synthon Hispania SL (2019) Public Assessment Report (Decentralised Procedure): Dasatinib Synthon Hispania 20 mg ; 50 mg ; 70 mg ; 80 mg ; 100 mg ; 140 mg Filmtabletten. https://file.wuxuwang.com/hma/DE_H_5896_003_PAR.pdf, available online (accessed: 2022-05-05)

[14] Furlong MT, Agrawal S, Hawthorne D, Lago M, Unger S, Krueger L, Stouffer B (2012) A validated LC-MS/MS assay for the simultaneous determination of the anti-leukemic agent dasatinib and two pharmacologically active metabolites in human plasma: application to a clinical pharmacokinetic study. Journal of pharmaceutical and biomedical analysis 58(1):130–5

[15] Araujo JC, Mathew P, Armstrong AJ, Braud EL, Posadas E, Lonberg M, Gallick GE, Trudel GC, Paliwal P, Agrawal S, Logothetis CJ (2012) Dasatinib combined with docetaxel for castration-resistant prostate cancer: results from a phase 1-2 study. Cancer 118(1):63–71

[16] Demetri GD, Lo Russo P, MacPherson IRJ, Wang D, Morgan JA, Brunton VG, Paliwal P, Agrawal S, Voi M, Evans TRJ (2009) Phase I dose-escalation and pharmacokinetic study of dasatinib in patients with advanced solid tumors. Clinical cancer research : an official journal of the American Association for Cancer Research 15(19):6232–40

[17] Takahashi S, Miyazaki M, Okamoto I, Ito Y, Ueda K, Seriu T, Nakagawa K, Hatake K (2011) Phase I study of dasatinib (BMS-354825) in Japanese patients with solid tumors. Cancer science 102(11):2058–64

[18] Meyer M, Schneckener S, Ludewig B, Kuepfer L, Lippert J (2012) Using expression data for quantification of active processes in physiologically based pharmacokinetic modeling. Drug metabolism and disposition: the biological fate of chemicals 40(5):892–901

[19] Scotcher D, Billington S, Brown J, Jones CR, Brown CDA, Rostami-Hodjegan A, Galetin A (2017) Microsomal and Cytosolic Scaling Factors in Dog and Human Kidney Cortex and Application for In Vitro-In Vivo Extrapolation of Renal Metabolic Clearance. Drug metabolism and disposition: the biological fate of chemicals 45(5):556–568

[20] Eriksson J, Solodenko J (2021) Building and evaluation of a PBPK model for Fluconazole in healthy adults. https://github.com/Open-Systems-Pharmacology/OSP-PBPK-Model-Library/tree/master/Fluconazole, available online (accessed: 2023-08-17)

[21] Wojtyniak JG, Selzer D, Schwab M, Lehr T (2021) Physiologically Based Precision Dosing Approach for Drug-Drug-Gene Interactions: A Simvastatin Network Analysis. Clinical pharmacology and therapeutics 109(1):201–211

[22] Shi P, Liao M, Chuang BC, Griffin R, Shi J, Hyer M, Fallon JK, Smith PC, Li C, Xia CQ (2018) Efflux transporter breast cancer resistance protein dominantly expresses on the membrane of red blood cells, hinders partitioning of its substrates into the cells, and alters drug-drug interaction profiles. Xenobiotica; the fate of foreign compounds in biological systems 48(11):1173–1183

[23] Prasad B, Evers R, Gupta A, Hop CECA, Salphati L, Shukla S, Ambudkar SV, Unadkat JD (2014) Interindividual variability in hepatic organic anion-transporting polypeptides and P-glycoprotein (ABCB1) protein expression: quantification by liquid chromatography tandem mass spectroscopy and influence of genotype, age, and sex. Drug metabolism and disposition: the biological fate of chemicals 42(1):78–88

[24] Hanke N, Frechen S, Moj D, Britz H, Eissing T, Wendl T, Lehr T (2018) PBPK Models for CYP3A4 and P-gp DDI Prediction: A Modeling Network of Rifampicin, Itraconazole, Clarithromycin, Midazolam, Alfentanil, and Digoxin. CPT: pharmacometrics & systems pharmacology 7(10):647–659

[25] Dallmann A, Solodenko J, Wendl T, Frechen S (2022) Building and Evaluation of a PBPK Model for Erythromycin in Healthy Adults. https://github.com/Open-Systems-Pharmacology/OSP-PBPK-Model-Library/blob/master/Erythromycin/Erythromycin_evaluation_report.pdf, available online (accessed: 2022-10-18)

[26] Nishimura M, Naito S (2006) Tissue-specific mRNA expression profiles of human phase I metabolizing enzymes except for cytochrome P450 and phase II metabolizing enzymes. Drug metabolism and pharmacokinetics 21(5):357–74

[27] Rodrigues AD (1999) Integrated cytochrome P450 reaction phenotyping: attempting to bridge the gap between cDNA-expressed cytochromes P450 and native human liver microsomes. Biochemical pharmacology 57(5):465–80

[28] Open Systems Pharmacology Suite Community (2018) PK-Sim® Ontogeny Database Documentation, Version 7.3. https://github.com/Open-Systems-Pharmacology/OSPSuite.Documentation/blob/master/PK-SimOntogenyDatabaseVersion7.3.pdf, available online (accessed: 2020-03-25)

[29] Nishimura M, Yaguti H, Yoshitsugu H, Naito S, Satoh T (2003) Tissue distribution of mRNA expression of human cytochrome P450 isoforms assessed by high-sensitivity real-time reverse transcription PCR. Yakugaku zasshi : Journal of the Pharmaceutical Society of Japan 123(5):369–75

[30] Rowland Yeo K, Walsky RL, Jamei M, Rostami-Hodjegan A, Tucker GT (2011) Prediction of time-dependent CYP3A4 drug-drug interactions by physiologically based pharmacokinetic modelling: impact of inactivation parameters and enzyme turnover. European journal of pharmaceutical sciences : official journal of the European Federation for Pharmaceutical Sciences 43(3):160–73

[31] Greenblatt DJ, von Moltke LL, Harmatz JS, Chen G, Weemhoff JL, Jen C, Kelley CJ, LeDuc BW, Zinny MA (2003) Time course of recovery of cytochrome p450 3A function after single doses of grapefruit juice. Clinical pharmacology and therapeutics 74(2):121–9

[32] Margaillan G, Rouleau M, Klein K, Fallon JK, Caron P, Villeneuve L, Smith PC, Zanger UM, Guillemette C (2015) Multiplexed Targeted Quantitative Proteomics Predicts Hepatic Glucuronidation Potential. Drug metabolism and disposition: the biological fate of chemicals 43(9):1331–5

[33] National Center for Biotechnology Information (NCBI) (2010) Expressed Sequence Tags (EST) from UniGene.

[34] Prasad B, Lai Y, Lin Y, Unadkat JD (2013) Interindividual variability in the hepatic expression of the human breast cancer resistance protein (BCRP/ABCG2): effect of age, sex, and genotype. Journal of pharmaceutical sciences 102(3):787–93

[35] Nishimura M, Naito S (2005) Tissue-specific mRNA expression profiles of human ATP-binding cassette and solute carrier transporter superfamilies. Drug metabolism and pharmacokinetics 20(6):452–77

[36] Deo AK, Prasad B, Balogh L, Lai Y, Unadkat JD (2012) Interindividual variability in hepatic expression of the multidrug resistance-associated protein 2 (MRP2/ABCC2): quantification by liquid chromatography/tandem mass spectrometry. Drug metabolism and disposition: the biological fate of chemicals 40(5):852–5

[37] Kolesnikov N, Hastings E, Keays M, Melnichuk O, Tang YA, Williams E, Dylag M, Kurbatova N, Brandizi M, Burdett T, Megy K, Pilicheva E, Rustici G, Tikhonov A, Parkinson H, Petryszak R, Sarkans U, Brazma A (2015) ArrayExpress update–simplifying data submissions. Nucleic acids research 43(Database issue):D1113–6

[38] Andre Dallmann (2021) IVIC with the particle dissolution module implemented in OSP. https://github.com/AndreDlm/IVIVC-with-particle-dissolution-module-in-OSP, available online (accessed: 2023-01-05)

[39] Developed by ChemAxon (2009) Chemicalize was used for prediction of dasatinib properties. https://chemicalize.com/, available online (accessed: 2022-05-03)

[40] Hořínková J, Šíma M, Slanař O (2019) Pharmacokinetics of Dasatinib. Prague medical report 120(2-3):52–63

[41] Tsume Y, Takeuchi S, Matsui K, Amidon GE, Amidon GL (2015) In vitro dissolution methodology, mini-Gastrointestinal Simulator (mGIS), predicts better in vivo dissolution of a weak base drug, dasatinib. European journal of pharmaceutical sciences : official journal of the European Federation for Pharmaceutical Sciences 76:203–12

[42] Watanabe R, Esaki T, Kawashima H, Natsume-Kitatani Y, Nagao C, Ohashi R, Mizuguchi K (2018) Predicting Fraction Unbound in Human Plasma from Chemical Structure: Improved Accuracy in the Low Value Ranges. Molecular pharmaceutics 15(11):5302–5311

[43] Wang L, Christopher LJ, Cui D, Li W, Iyer R, Humphreys WG, Zhang D (2008) Identification of the human enzymes involved in the oxidative metabolism of dasatinib: an effective approach for determining metabolite formation kinetics. Drug metabolism and disposition: the biological fate of chemicals 36(9):1828–39

[44] Chang M, Bathena S, Christopher LJ, Shen H, Roy A (2022) Prediction of drug-drug interaction potential mediated by transporters between dasatinib and metformin, pravastatin, and rosuvastatin using physiologically based pharmacokinetic modeling. Cancer chemotherapy and pharmacology 89(3):383–392

[45] Pahwa S, Alam K, Crowe A, Farasyn T, Neuhoff S, Hatley O, Ding K, Yue W (2017) Pretreatment With Rifampicin and Tyrosine Kinase Inhibitor Dasatinib Potentiates the Inhibitory Effects Toward OATP1B1- and OATP1B3-Mediated Transport. Journal of pharmaceutical sciences 106(8):2123–2135

[46] Open Systems Pharmacology Suite Community (2021) Open Systems Pharmacology Suite Manual. https://raw.githubusercontent.com/Open-Systems-Pharmacology/OSPSuite.Documentation/master/OpenSystemsPharmacologySuite.pdf, available online (accessed: 2023-05-04)

[47] Fisher RS, Rock E, Malmud LS (1987) Effects of meal composition on gallbladder and gastric emptying in man. Digestive diseases and sciences 32(12):1337–44

[48] Schmitt W (2008) General approach for the calculation of tissue to plasma partition coefficients. Toxicology in vitro : an international journal published in association with BIBRA 22(2):457–67

[49] ChemicalBook (2006) ChemicalBook was used for collection of chemical information of dasatinib. https://www.chemicalbook.com/, available online (accessed: 2023-01-05)

[50] Eley T, Luo FR, Agrawal S, Sanil A, Manning J, Li T, Blackwood-Chirchir A, Bertz R (2009) Phase I study of the effect of gastric acid pH modulators on the bioavailability of oral dasatinib in healthy subjects. Journal of clinical pharmacology 49(6):700–9

[51] Yago MR, Frymoyer A, Benet LZ, Smelick GS, Frassetto LA, Ding X, Dean B, Salphati L, Budha N, Jin JY, Dresser MJ, Ware JA (2014) The use of betaine HCl to enhance dasatinib absorption in healthy volunteers with rabeprazole-induced hypochlorhydria. The AAPS journal 16(6):1358–65

[52] Johnson FM, Agrawal S, Burris H, Rosen L, Dhillon N, Hong D, Blackwood-Chirchir A, Luo FR, Sy O, Kaul S, Chiappori AA (2010) Phase 1 pharmacokinetic and drug-interaction study of dasatinib in patients with advanced solid tumors. Cancer 116(6):1582–91

[53] Okada M, Yao T, Sakurai T, Arita M, Okabe N, Iida M, Okada Y, Koga T (1992) A comparative study of once-a-day morning and once-a-day bedtime administration of 40 mg famotidine in treating gastric ulcers. The American journal of gastroenterology 87(8):1009–13

[54] Dennis L Decktor, Malcolm Robinson SG (1995) Comparative Effects of Liquid Antacids on Esophageal and Gastric pH in Patients with Heartburn. American journal of therapeutics 2(7):481–486

[55] Guest EJ, Aarons L, Houston JB, Rostami-Hodjegan A, Galetin A (2011) Critique of the two-fold measure of prediction success for ratios: application for the assessment of drug-drug interactions. Drug metabolism and disposition: the biological fate of chemicals 39(2):170–3

[56] Fuhr LM, Marok FZ, Hanke N, Selzer D, Lehr T (2021) Pharmacokinetics of the CYP3A4 and CYP2B6 Inducer Carbamazepine and Its Drug-Drug Interaction Potential: A Physiologically Based Pharmacokinetic Modeling Approach. Pharmaceutics 13(2):1–21

[57] Wendl T, Frechen S, Solodenko J, Dallmann A (2021) Building and Evaluation of a PBPK Model for Efavirenz in Healthy Adults. https://github.com/Open-Systems-Pharmacology/OSP-PBPK-Model-Library/blob/master/Efavirenz/efavirenz_evaluation_report.pdf, available online (accessed: 2022-10-18)

[58] Britz H, Hanke N, Volz AK, Spigset O, Schwab M, Eissing T, Wendl T, Frechen S, Lehr T (2019) Physiologically-Based Pharmacokinetic Models for CYP1A2 Drug–Drug Interaction Prediction: A Modeling Network of Fluvoxamine, Theophylline, Caffeine, Rifampicin, and Midazolam. CPT: Pharmacometrics and Systems Pharmacology 8(5):296–307

[59] Fuhr LM, Marok FZ, Fuhr U, Selzer D, Lehr T (2023) Physiologically based pharmacokinetic modeling of bergamottin and 6,7-dihydroxybergamottin to describe CYP3A4 mediated grapefruit-drug interactions. Clinical pharmacology and therapeutics (031):0–2

[60] Marok FZ, Wojtyniak JG, Fuhr LM, Selzer D, Schwab M, Weiss J, Haefeli WE, Lehr T (2023) A Physiologically Based Pharmacokinetic Model of Ketoconazole and Its Metabolites as Drug–Drug Interaction Perpetrators. Pharmaceutics 15(2)

[61] Li X, Frechen S, Moj D, Lehr T, Taubert M, Hsin CH, Mikus G, Neuvonen PJ, Olkkola KT, Saari TI, Fuhr U (2020) A Physiologically Based Pharmacokinetic Model of Voriconazole Integrating Time-Dependent Inhibition of CYP3A4, Genetic Polymorphisms of CYP2C19 and Predictions of Drug-Drug Interactions. Clinical pharmacokinetics 59(6):781–808

[62] Li X, He Y, Ruiz CH, Koenig M, Cameron MD, Vojkovsky T (2009) Characterization of dasatinib and its structural analogs as CYP3A4 mechanism-based inactivators and the proposed bioactivation pathways. Drug metabolism and disposition: the biological fate of chemicals 37(6):1242–50